

THESIS

MODELING IN A THREE-DIMENSIONAL WORLD:
WHITEWATER PARK HYDRAULICS AND THEIR IMPACT ON
AQUATIC HABITAT IN COLORADO

Submitted by

Eleanor Kolden

Department of Civil and Environmental Engineering

In partial fulfillment of the requirements

For the Degree of Master of Science

Colorado State University

Fort Collins, Colorado

Spring 2013

Master's Committee:

Advisor: Brian P. Bledsoe

Ellen Wohl
Neil S. Grigg

ABSTRACT

MODELING IN A THREE-DIMENSIONAL WORLD: WHITEWATER PARK HYDRAULICS AND THEIR IMPACT ON AQUATIC HABITAT IN COLORADO

Whitewater parks (WWPs) are becoming more popular in Colorado rivers and streams, but the effects of WWPs on aquatic habitat and fish passage are poorly understood. This study investigated the use of a three-dimensional (3-D) hydrodynamic model (FLOW-3D[®]) for assessing effects of WWPs on aquatic habitat. The objective of this study was to compare modeled habitat quality to actual fish biomass and to examine the utility of 3-D modeling (vs. two-dimensional (2-D) modeling) in this hydraulically-complex system. Two sections of a small river in Colorado were modeled: one natural section, and one section containing a WWP with three engineered drop structures. A 2-D habitat suitability analysis for juvenile and adult brown and rainbow trout, longnose dace, and longnose sucker predicted higher habitat quality in the WWPs than the natural reaches for adult brown and rainbow trout at some flow rates, while in-stream surveys showed higher fish biomass per volume in the natural pools. All hydraulic metrics (depth, depth-averaged velocity, turbulent kinetic energy (TKE), 2-D vorticity, and 3-D vorticity) had higher magnitudes in the WWP pools than in the natural pools. In the WWP pools, 2-D model results did not describe the spatial distribution of flow characteristics or the magnitude of variables as well as 3-D results. This thesis supports the use of 3-D modeling for complex flow found in WWPs, but other projects should be evaluated case-by-case to determine if the simplified 2-D rendering of flow characteristics is acceptable. For 3-D modeling to be widely useful, improved understanding of linkages between 3-D aquatic habitat quality and hydraulic descriptors such as TKE, vorticity, and velocity is needed.

ACKNOWLEDGMENTS

I would like to give a huge thanks to my colleague Brian Fox for spearheading this research, my advisor Brian Bledsoe for his help throughout, Matt Kondratieff at Colorado Parks and Wildlife (CPW), Ellen Wohl and Neil Grigg for being my committee members and inspiring teachers, my parents for their endless support, David for his tireless encouragement and editing help, CPW and Colorado Water Institute (CWI) for funding support, Jeff Burnham at Flow Science, Ashley Ficke, Dan Gessler, and Bill Miller.

TABLE OF CONTENTS

ABSTRACT.....	ii
ACKNOWLEDGMENTS	iii
LIST OF TABLES	vi
LIST OF FIGURES	vii
LIST OF SYMBOLS	ix
UNITS OF MEASURE.....	x
CHAPTER 1 INTRODUCTION.....	1
CHAPTER 2 METHODS.....	7
2.1 Site Description	7
2.2 Species of Interest.....	9
2.3 Bathymetric and Hydrologic Surveys	9
2.4 Numerical Hydraulic Modeling.....	10
2.5 Model Validation.....	13
2.6 Vorticity Calculations.....	14
2.7 Reach Extents	15
2.8 2-D Habitat Modeling.....	16
CHAPTER 3 RESULTS.....	18
3.1 2-D and 3-D Hydraulic Variables.....	18
3.1.1 Depth	18
3.1.2 Velocity	19
3.1.3 TKE	21
3.1.4 Vorticity.....	22

3.2	3-D Flow Patterns.....	28
3.3	2-D Habitat Modeling.....	28
3.3.1	Juvenile Brown Trout.....	30
3.3.2	Adult Brown Trout.....	30
3.3.3	Juvenile Rainbow Trout.....	32
3.3.4	Adult Rainbow Trout.....	32
3.3.5	Longnose Dace.....	35
3.3.6	Longnose Sucker.....	36
CHAPTER 4 CASE STUDY: BIOMASS SURVEYS.....		37
CHAPTER 5 DISCUSSION.....		41
5.1	Hydraulic Variables.....	41
5.2	2-D Habitat Models.....	44
5.3	Future Implications.....	46
CHAPTER 6 CONCLUSION.....		48
BIBLIOGRAPHY.....		49
APPENDIX A DETAILED NUMERICAL MODELING METHODS.....		54
LIST OF ABBREVIATIONS.....		57

LIST OF TABLES

Table 2.1. Discharges used for simulating validation conditions and habitat modeling conditions.....	12
Table 3.1. Maximum flow depth (m) in WWP pools and natural pools at all flow rates.....	18
Table 3.2. Maximum depth-averaged velocity (m/s) in WWP pools and natural pools at all flow rates.	19
Table 3.3. Maximum TKE (m^2/s^2) in WWP pools and natural pools for all flow rates.	21
Table 3.4. Maximum (a) 3-D and (b) 2-D vorticity (s^{-1}) in WWP pools and natural pools for all flow rates.....	23
Table 3.5. Percentage of pool area with good habitat ($HSI > 0.5$) for each species life stage and flow rate. Grey highlight indicates significant differences between WWP pools and natural pools ($p < 0.05$ for Wilcoxon and t -test).....	29
Table A.1. Cell size in FLOW-3D computational mesh for WWP reaches and natural reaches at all flow rates.....	55

LIST OF FIGURES

Figure 2.1. Map of study site.	8
Figure 3.1. Flow depth (m) in pools: (a) WWP2 and (b) NR3 at 4.25 cms. The pool in the natural reach starts just below the protruding boulder on the left bank.	19
Figure 3.2. Depth-averaged velocity (m/s) in pools: (a) WWP2 and (b) NR3 at 4.25 cms.	20
Figure 3.3. Cross-sections showing the downstream velocity component (m/s) in pools: (a) WWP2 and (b) NR3 at 4.25 cms.	21
Figure 3.4. Cross-sections showing TKE (m^2/s^2) in pools: (a) WWP2 and (b) NR3 at 4.25 cms.	22
Figure 3.5. Cross-sections showing 3-D vorticity (s^{-1}) in pools: (a) WWP2 and (b) NR3 at 4.25 cms.	23
Figure 3.6. Plan view of WWP2 pool just below water surface at 4.25 cms: (a) color contours represent 3-D vorticity values (s^{-1}) and arrows represent direction of flow in the horizontal (XY) plane, and (b) color contours represent absolute value of 2-D vorticity values (s^{-1}).	25
Figure 3.7. Plan view of WWP2 pool 0.6 m below water surface at 4.25 cms: (a) color contours represent 3-D vorticity values (s^{-1}) and arrows represent direction of flow in the horizontal (XY) plane, and (b) color contours represent absolute value of 2-D vorticity values (s^{-1}).	26
Figure 3.8. Plan view of WWP2 pool 1.2 m below water surface and just above channel bed at 4.25 cms: (a) color contours represent 3-D vorticity values (s^{-1}) and arrows represent direction of flow in the horizontal (XY) plane, and (b) color contours represent absolute value of 2-D vorticity values (s^{-1}).	27

Figure 3.9. Streamlines showing patterns of flow in pools: (a) WWP2 and (b) NR3 at 4.25 cms. Coloring represents velocity magnitude (m/s).	28
Figure 3.10. Habitat suitability results for adult brown trout in: (a) WWP pools and (b) natural pools.	31
Figure 3.11. Average good adult brown trout habitat as a percentage of wetted area for low, medium, and high flow rates. Stars indicate significant differences in amount of habitat between WWP pools and natural pools.	32
Figure 3.12. Habitat suitability results for adult rainbow trout in: (a) WWP pools and (b) natural pools.	34
Figure 3.13. Average good adult rainbow trout habitat as a percentage of wetted area for low, medium, and high flow rates. Stars indicate significant differences in amount of habitat between WWP pools and natural pools.	35
Figure 4.1. Adult brown trout biomass normalized by pool surface area: (a) biomass in each pool in 2010, (b) biomass in each pool in 2012, and (c) average biomass in WWP pools and natural pools in 2010 and 2012. Error bars represent 95% confidence intervals.	39
Figure 4.2. Adult brown trout biomass normalized by pool volume: (a) biomass in each pool in 2010, (b) biomass in each pool in 2012, and (c) average biomass in WWP pools and natural pools in 2010 and 2012. Error bars represent 95% confidence intervals.	40
Figure A.1. Three ways of representing roughness in CFD models (from Olsen and Stokseth [1995]).	56

LIST OF SYMBOLS

\hat{i}	unit vector in the x-direction
\hat{j}	unit vector in the y-direction
\hat{k}	unit vector in the z-direction
u	x-component of velocity (m/s)
v	y-component of velocity (m/s)
w	z-component of velocity (m/s)
x	downstream (longitudinal) direction of flow (m)
y	cross-stream (latitudinal) direction of flow (m)
z	vertical direction of flow (m)
$\bar{\xi}_{3D}$	3-D vorticity vector (s^{-1})
$\bar{\xi}_{2D}$	2-D vorticity vector (s^{-1})
σ	standard deviation

UNITS OF MEASURE

cm	centimeter(s)
cms	cubic meter(s) per second
km	kilometer(s)
km ²	square kilometer(s)
m	meter(s)
m/s	meter(s) per second
m ²	square meter(s)
m ² /s ²	square meter(s) per second squared
mm	millimeter(s)
%	percent
s ⁻¹	inverse second(s)

CHAPTER 1 INTRODUCTION

Hydraulic conditions in lotic systems are one of many important factors influencing stream ecosystem health and function [Lamouroux *et al.*, 1995]. Flow patterns and characteristics influence habitat in many ways, by creating cover, influencing oxygen availability, regulating water temperature, and shaping channel morphology. River engineering projects, such as dam construction, dredging, channelization, or addition of in-stream habitat structures clearly create changes in these hydraulic conditions [Roni and Beechie, 2013]. It is not always clear how such structural changes may positively or negatively affect habitat quality for aquatic organisms.

For the last three decades, researchers have studied the effects of hydraulic conditions on habitat quality using the Physical HABitat SIMulation (PHABSIM) model and other hydrodynamic modeling processes [Booker *et al.*, 2004; Bovee, 1982]. In most studies, depth and depth-averaged velocity are the primary hydraulic variables used; which were first formally correlated to habitat quality by Bovee [1982]. Hydraulic models have also been used to assess the effects of in-stream wood and rock habitat structures on aquatic habitat quality (e.g., Lacey and Millar [2004]).

The importance of other hydraulic variables, such as turbulence, vorticity, circulation, velocity gradients, and kinetic energy gradients, has only recently been examined. Turbulence is a measurement of rapid velocity fluctuations and can increase fish swimming cost, but can also trigger important migratory movements, among other effects [Silva *et al.*, 2012]. Vorticity and circulation describe flow complexity, but it is unknown how specific organisms react to different amounts of flow complexity [Crowder and Diplas, 2002]. Velocity gradients and kinetic energy gradients describe spatially-varying flow that influences where a fish chooses to travel, feed, or

rest; but again, the exact effects of different gradient scales on specific fish species is unknown [Crowder and Diplas, 2000a]. Much more research is necessary before clear correlations can be made between these variables and habitat quality [Kozarek *et al.*, 2010].

As with the construction of other types of channel-spanning hydraulic structures, whitewater parks (WWPs) result in significant changes to hydraulic conditions by altering flow patterns, depth, velocity, and general flow complexity. WWPs are primarily used for whitewater kayaking and recreational tubing and have become very popular in Colorado, where at least twelve parks currently exist and several more are in the design and construction stages [RipBoard, 2011]. WWPs are constructed by building wing walls on the channel banks with large permanent boulders. The walls create a lateral constriction and typically force flow through a chute near mid-channel. This chute has a substantial drop in elevation, similar to a small spillway or weir, and a plunge pool is created just downstream. A standing wave is created at the top of the plunge pool where boaters can surf and perform tricks. The orientation of the wing walls also creates large lateral eddies in the pools immediately downstream. These eddies can be used for boaters to rest, and also provide a slow water area for fishing and swimming. WWP construction is often coupled with broader river-improvement projects, including aesthetic enhancement, riparian vegetation planting, or ecological rehabilitation [McGrath, 2003].

It is widely assumed that the installation of these recreational structures has a positive effect on aquatic habitat quality because it increases pool area, which is a key component of healthy salmonid habitat and is often a primary goal of habitat-improvement projects in the United States [Larscheid and Hubert, 1992; Roni *et al.*, 2008]. Deeper pools are beneficial to fish because they provide essential habitat during very low flows [Binns, 1994]. Also, researchers in Norway found that brown trout had higher growth rates in deeper pools and higher daytime use of deeper pools [Greenberg and Giller, 2001; Greenberg *et al.*, 2001]. Designers of WWPs

generally assume they are adding structures similar to engineered habitat-enhancement structures, such as cross vanes and j-hooks, and that WWPs should confer similar positive effects on aquatic habitat [McGrath, 2003]; however, this assumption has yet to be demonstrated and tested rigorously.

To assess the effects of altered hydraulic conditions found in WWPs or similar habitat enhancements, it is necessary to describe the hydraulic conditions associated with such structures accurately. Descriptive methods include field-based measurements, physical modeling, and numerical modeling. Field-based measurements can provide very accurate snapshots of real-world conditions; however, it is rarely feasible to collect data representing every possible condition. Accessibility and safety concerns, inclement weather, equipment limitations, and the limited availability of staff time, expertise, or project funding often hinder data-collection efforts. Physical models, on the other hand, allow data collection over a range of conditions by running multiple flows through a scale model of the natural system. Physical models require a large space and can be expensive and time-consuming to build [Olsen and Stokseth, 1995]. Numerical modeling also provides estimates of hydraulic characteristics over a range of conditions using computer-based simulations. Numerical models may be one-dimensional (1-D), two-dimensional (2-D), or three-dimensional (3-D); with 1-D modeling representing only longitudinal (downstream) flow, 2-D adding the lateral flow component, and 3-D including the vertical flow component [Crowder and Diplas, 2000a]. Numerical modeling allows for the representation of an infinite number of conditions beyond the range measurable in the field [Booker *et al.*, 2004]. The primary limitations are computational power and software cost, which though significant, can potentially be less than those associated with physical models and added field-based sampling.

It is important to identify the flow features of interest in each specific project and choose a descriptive method that accurately describes those features [Crowder and Diplas, 2000a]. For example, a large boulder may create a localized flow alteration, but may not affect the average flow conditions through the reach. If the goal of a study is to understand the flow around the boulder, then the model chosen must have enough 1-D, 2-D, or 3-D resolution to obtain the desired information [Crowder and Diplas, 2000b]. One-dimensional and 2-D numerical modeling has been successfully applied to many natural river systems [Booker and Dunbar, 2004; Ghanem *et al.*, 1996; Lacey and Millar, 2004], but understanding 3-D hydraulics is important in systems with a substantial vertical flow component, such as WWPs [Lane *et al.*, 1999], and in systems where there are complex horizontal and vertical velocity gradients [Booker *et al.*, 2004]. While hydraulic models are often used for the design of structures, the results of these models are generally not shared with resource agency personnel and the public. As a result, very little is known about how the specific design elements commonly incorporated into WWP designs affect flow patterns, velocity, and flow complexity.

There are currently no published studies specifically addressing the effects of WWPs on aquatic habitat. Also, there are few (if any) published studies using 3-D modeling to simulate modifications of fish habitat. Habitat modeling, though common in natural and restored river reaches [Booker and Dunbar, 2004; Lacey and Millar, 2004], has not occurred in any published WWP studies. The primary limitation to research on this topic is that ecological functions important for assessing habitat have not been correlated to 3-D hydrodynamics [Pasternack *et al.*, 2008].

Two-dimensional models of habitat quality can be a powerful and important tool for managers. They do, however, come with several important limitations. Habitat Suitability Indices (HSI) are based solely on the 2-D hydraulic variables of depth and depth-averaged

velocity. Cover and substrate are included in the analysis for some species and life stages. There are clearly many other non-hydraulic factors that will influence aquatic habitat, including those associated with water quality (turbidity, temperature, etc.), food availability, and biotic interactions (competition, predation, etc.) [Booker *et al.*, 2004]. Additionally, there are numerous hydraulic variables not included in HSI analysis, including turbulence, vorticity, and circulation—many of which cannot be accurately simulated in a 2-D environment. The 2-D simplification of hydraulic results ignores the effects of vertical velocity components and gradients within the water column [Crowder and Diplas, 2000a]. HSI equations are parameterized based on either field measurements or expert opinion to model the conditions ideal for fish habitation. In cases where field measurements are used, an assumption is made that the fish under observation have chosen their locations in a river channel because those locations exhibit ideal conditions. This assumption often fails, especially for juvenile fish or smaller species that may not have access to prime locations as a result of competition by larger and more aggressive fish [Shuler and Nehring, 1993]. Additionally, the validity of HSI models are limited by the range of conditions used to parameterize them. The models will most accurately predict conditions similar to those observed in the field during surveys. Extrapolation of the models to conditions outside the range of calibration can lead to reduced prediction accuracy. For example, it is possible that a survey could indicate adult brown trout occupying habitats with velocities up to 1.7 m/s, but if those were the fastest flows observed on that day, it remains uncertain whether adult brown trout could inhabit faster flows.

The final problem with current research is that there are no published studies that survey on-the-ground biological or ecological conditions to evaluate the actual impacts of WWPs. This lack of information creates a problem for state wildlife agency personnel, who are asked to

comment on the 404 permits required for WWP construction. They must provide their expert opinion without having any concrete studies to inform that opinion.

This research addresses some of the gaps and limitations present when modeling the hydraulics and habitat of WWPs, using a 3-D modeling environment to better characterize and predict the complex 3-D nature of aquatic habitat. Specifically, the research objectives are as follows:

- 1) describe and compare fish habitat quality in WWPs and natural reaches using a traditional method based on 2-D hydraulic modeling and habitat suitability criteria;
- 2) compare predicted fish habitat quality to results from field surveys that provide preliminary estimates of fish biomass;
- 3) use 3-D modeling to describe and compare ecologically-relevant hydraulic descriptors in WWPs versus natural reaches;
- 4) compare 2-D and 3-D hydraulic and habitat modeling results and examine whether 3-D modeling is justified for assessing habitat quality in WWPs; and
- 5) present future applications and research directions for 3-D hydraulic modeling and habitat quality assessment in complex river settings such as WWPs.

This study does not specifically address the topic of fish passage, which is a common concern pertaining to WWPs. Fish passage is clearly a valid concern, due to the constricted high-velocity flows found in WWP structures, and will be addressed in a forthcoming publication [Fox, in prep].

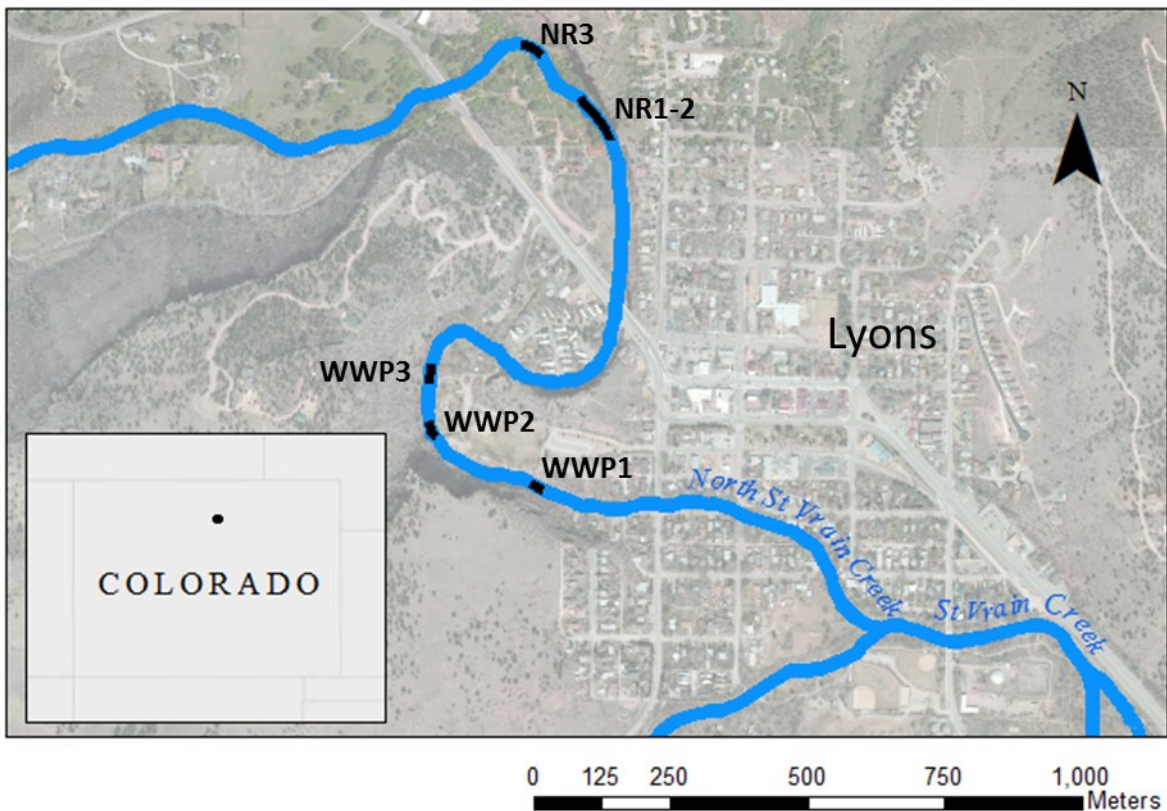
CHAPTER 2 METHODS

2.1 Site Description

North St. Vrain Creek originates in the Rocky Mountains (near St. Vrain Mountain) on the east side of the Continental Divide in Northern Colorado. It drains an area of 322 km², which is mostly forested with some suburban development at the lower elevations. The creek has snowmelt hydrology with peak flows in early summer, but is highly regulated by upstream dams and diversions. The study site is within the Town of Lyons, just before the confluence with South St. Vrain Creek. The creek in this vicinity has a slope of 1% with a channel bed primarily made of boulders and cobbles underlain by Lyons sandstone. The entire study reach has steep sandstone cliffs bordering one side of the creek. The channel morphology is naturally composed of riffles, runs, and shallow pools. In a typical year, the flow varies between 0.1 and 11 cms.

The study design consisted of two sections of the North St. Vrain (Figure 2.1). The WWP section was within Meadow Park in downtown Lyons, a 400-m reach where nine WWP drop structures were installed in 2003. Three drop structures were selected for hydraulic modeling, one at the downstream end of the reach, one near the middle, and one at the very upstream end of the reach. Each modeled reach was approximately 50-m long and included the upstream approach to the drop, the drop itself, and the pool downstream of the drop. Hereafter, these reaches will be referred to as ‘WWP reaches.’ The natural section of the study was 1,000-m long and was located about 1 km upstream of the WWP section on private property, where there had been limited in-stream engineering or channel manipulation. To simplify surveying and modeling, one long reach (~75 m) at the downstream end of the natural section and one shorter reach (~40 m) at the upstream end were modeled, and then each broken into smaller reaches for analysis. These reaches will be referred to as ‘natural reaches.’ It is important to note that

although these reaches are termed ‘natural reaches’ in this study, it is only because they are more natural than the WWP reaches. They have still been affected heavily by upstream flow alteration and water withdrawals. Due to the location of these reaches on private property, there has also been small-scale in-channel manipulation, primarily moving small rocks for aesthetic and recreational purposes.



Note: Reach NR1-2 includes NR1-A, NR1-B, and NR2

Figure 2.1. Map of study site.

The Lyons WWP was chosen for this study because Colorado Parks and Wildlife (CPW) was already studying fish biomass and movement in the North St. Vrain. Also, there are different types of WWP drop structures within the park, some with steeper, narrower chutes, and some with less-constricted free overfalls, which allow for a more diverse analysis of WWP effects. Compared to other WWPs in Colorado, the Lyons park is fairly small. With peak runnable flows

around 14.5 cms, it is much smaller than other popular parks found in the cities of Salida, Golden, and Glenwood Springs, which have peak runnable flows ranging from 28 to 425 cms.

2.2 Species of Interest

The most abundant fish species in this stretch of the North St. Vrain is brown trout (*Salmo trutta*). Brown trout are not native to Colorado, but have naturalized self-sustaining populations in many of the state's rivers [Belica, 2007]. Brown trout are regulated as a game fish in the state and are stocked in many areas, though not in the North St. Vrain. Adult brown trout are largely piscivorous and move upstream to spawn in fall and winter [Raleigh *et al.*, 1986]. Rainbow trout (*Oncorhynchus mykiss*) are another common non-native species in the North St. Vrain. Rainbow trout usually spawn in spring, but hatchery populations can spawn at other times of the year as well [Raleigh *et al.*, 1984]. Rainbow trout primarily feed on drifting insects and will eat other food occasionally [Bernstein and Montgomery, 2008]. Longnose dace (*Rhinichthys cataractae*) and longnose sucker (*Catostomus catostomus*) are two species of Colorado native fish included in this study. Longnose dace prefer shallow flows, are adapted for bottom-feeding, and spawn in riffles in early summer [Edwards *et al.*, 1983]. Longnose suckers move upstream to spawn in early summer and prefer areas with moderate current [Edwards, 1983].

2.3 Bathymetric and Hydrologic Surveys

Bathymetry data were collected in the form of XYZ coordinates using a ground-based Light Detection and Ranging (LIDaR) system, a Leica Total Station, and a Topcon[®] HiPer XT™ Global Positioning System (GPS) base and rover system. Ground-based LIDaR records high-resolution topography data, but does not penetrate water, so LIDaR surveying was conducted during winter low flows to obtain as much above-water data as possible. The total station and GPS system were used to survey underwater cross-sections in areas of low bathymetric

variability. Where there was high variability, breaklines and extra points were surveyed to increase resolution. Areas of high variability identified for intensive surveying were defined following Crowder and Diplas [2000b] as having features that visibly significantly affected flow patterns. Underwater data resolution varied from approximately eight points per square meter (with the hand-held GPS) to 10,000 points per square meter (with ground-based LIDaR). Though some areas had lower survey resolution, the survey still incorporated all of the important topographic variability. Point data from the surveys were integrated into a continuous 3-D surface using the design software Geomagic Studio[®]. Measured hydrologic data included water surface elevation, wetted perimeter location, and velocity profiles. Elevation and location measurements were conducted using the same total station and GPS system used for bathymetry surveys. Velocity profiles were measured using an acoustic Doppler velocimeter (ADV) and a Marsh McBirney flow meter.

2.4 Numerical Hydraulic Modeling

The 3-D computation fluid dynamics (CFD) software FLOW-3D[®] v10.0 (hereafter referred to as FLOW-3D) was used to model each of the reaches. The CFD process uses the fluid equations of motion to solve Reynolds-Averaged Navier-Stokes (RANS) equations that describe fluid flow. FLOW-3D was chosen for this study over other 3-D CFD software packages because of its efficacy in accurately representing free-surface systems such as natural river channels. FLOW-3D uses Cartesian coordinates to create a hexahedral grid, also called a mesh, in the computational domain. The program uses a process called volume of fluid (VOF) to accurately represent the free surface within this structured mesh [Flow Science, 2009]. The default renormalization group (RNG) turbulence closure with dynamically-computed turbulent mixing length was used in this study.

FLOW-3D requires boundary conditions at six locations in the computational mesh. The top boundary was set as a symmetry boundary, while the side and bottom boundaries were set as solid walls. Each of these boundaries was well outside of the area of flow. A volumetric flow rate was measured for each reach and used for the upstream boundary. The channel bed was artificially extended upstream approximately 5 m so that the flow would be steady before it entered the actual reach. Because there were no diversions or tributaries in the area of study, discharge was assumed to be constant throughout each reach. The downstream boundary was a specified pressure boundary, and was specified based on the measured water surface elevation at the downstream end of each reach.

Five different flow rates were simulated for each modeled reach. Two of these flow rates were used to validate the model (described in Section 2.5 *Model Validation*), and three were used for habitat analysis. The habitat analysis flow rates mimicked ecologically significant low, medium, and high flow rates for the species in this region. During brown trout spawning in the fall, flow in the North St. Vrain is typically very low. Low flow persists through the winter and into the spring period of rainbow trout spawning, and is important for the overwintering habitat of all species. Hydraulic models were run at 0.42 cms to simulate these important low flows. As snowmelt starts in the spring, flow increases and fish begin feeding more [Belica, 2007]. Hydraulic models were run at 4.25 cms to simulate this medium flow. At the peak of runoff, in early summer, all species must be able to find refugia to avoid expending too much energy or being swept downstream. Hydraulic models were run at 8.5 cms to simulate this high flow. All of the simulated flow rates are summarized in Table 2.1.

Table 2.1. Discharges used for simulating validation conditions and habitat modeling conditions.

Reach	Validation Flow Rate (cms)	Habitat Flow Rate (cms)		
		Low	Medium	High
WWP1	0.79, 4.76	0.42	4.25	8.5
WWP2	0.25, 4.87	0.42	4.25	8.5
WWP3	0.79, 4.79	0.42	4.25	8.5
NR1-2 ^a	1.02, 2.66	0.42	4.25	8.5
NR3	0.25, 2.21	0.42	4.25	8.5

^a Reach NR1-2 includes NR1-A, NR1-B, and NR2

Each simulation used a structured rectangular mesh that was incrementally refined until the solution was grid-independent (meaning that a smaller mesh size would no longer appreciably affect the simulation output). Final uniform grid sizes ranged from 3.81 to 15.24 cm, depending on the reach and flow rate, and the number of active cells ranged from 1 to 3 million.

The surveyed bathymetry data were converted into a stereolithography (STL) file and imported into FLOW-3D as a solid 3-D object. Because of the detailed topographic surveys, it was assumed that channel roughness elements in the WWP reaches were adequately resolved in the STL file. Through the model validation process (described in Section 2.5 *Model Validation*), this assumption was shown to be acceptable. The reason this assumption could be made for the WWP reaches is that the flow over the drop structure, which is the primary area of hydraulic control and interest, is grouted and has very little physical roughness. In contrast, the natural reaches have substantial roughness for the entire length, so the assumption did not hold. In these reaches it was necessary to model the roughness using a porous region near the bed [Carney *et al.*, 2006]. For a more-detailed description of model specifications, roughness approximations, and sensitivity analyses, please see Appendix A.

All post processing of hydraulic results (except habitat suitability calculations) was performed using EnSight[®] Standard v10.0.2.

2.5 Model Validation

In order to validate the 3-D modeling results, modeled variables were compared to the same variables measured in the field. As described above, measured hydrologic variables included water surface elevation, wetted perimeter, and velocity profiles. Hydrologic measurements occurred at low flow (~0.3 cms) and medium flow (~4.25 cms). Because the 2011-2012 water year was very dry, it was not possible to obtain validation data at high flow (~8.5 cms).

Model validation simulations were performed for each reach at the same two flow rates for which hydrologic variables were measured (Table 2.1). Results were compared to measured conditions using velocity profiles, water surface elevation, wetted perimeter, and observed locations of hydraulic features such as eddies and jumps. In the WWP reaches, the primary area of concern was the flow over each drop structure. In every reach, the flow profiles matched up very closely, with a maximum distance of 3 cm between the measured and modeled water surface profiles. Using a survey rod to measure water surface elevation adds a potential error of at least ± 2 cm, so these results are well within the range of acceptable results. In the downstream pools, modeled water surface elevations differed by less than 1 cm from the measured elevations. The modeled velocity profiles in the three WWP validation simulations, where velocity was measured, had error of less than 16%; which is within acceptable error rates based on previous studies [Kozarek *et al.*, 2010].

In the natural reaches, the error in water surface elevations was less than 5 cm and it was determined that this amount of error was acceptable. Velocity profiles were not measured in the natural reaches, though the modeled velocities were deemed reasonable based on knowledge of the site.

Validation data for the flow within the pools were also obtained from CPW field measurements using an acoustic Doppler current profiler (ADCP). Surveyors measured velocities at cross-sections in all the WWP reaches and natural reaches, and the velocity magnitudes and distributions they found match closely with the modeled conditions found through the use of FLOW-3D.

2.6 Vorticity Calculations

Vorticity is a vector that represents the rate of rotation of a small fluid element around its axes [Crowder and Diplas, 2002]. In the case of 3-D flow, particles will be rotating around the x , y , and z axes. In uniform flow, particles experience translation and/or linear or angular deformation, but will not experience rotation, thus vorticity is zero. The complex and non-uniform flow patterns that are often found in natural channels create flow complexity, and have non-zero vorticity values, making vorticity a physically-meaningful metric to describe flow complexity [Crowder and Diplas, 2002].

Three-dimensional vorticity can be described by the following equation:

$$\bar{\xi}_{3D} = \left(\frac{\partial w}{\partial y} - \frac{\partial v}{\partial z} \right) \hat{i} + \left(\frac{\partial u}{\partial z} - \frac{\partial w}{\partial x} \right) \hat{j} + \left(\frac{\partial v}{\partial x} - \frac{\partial u}{\partial y} \right) \hat{k} \quad (2.1)$$

where

- $\bar{\xi}_{3D}$ = 3-D vorticity vector (s^{-1});
- \hat{i} = unit vector in the x -direction;
- \hat{j} = unit vector in the y -direction;
- \hat{k} = unit vector in the z -direction;
- u = x -component of velocity (m/s);
- v = y -component of velocity (m/s);
- w = z -component of velocity (m/s);

- x = downstream (longitudinal) direction of flow (m);
- y = cross-stream (latitudinal) direction of flow (m); and
- z = vertical direction of flow (m).

The right-hand side of the equation represents the curl of the velocity vector. Three-dimensional vorticity is always positive. To calculate vorticity in a 2-D (depth-averaged) flow field, there is no z velocity and the equation simplifies to:

$$\bar{\xi}_{2D} = \left(\frac{\partial v}{\partial x} - \frac{\partial u}{\partial y} \right) \hat{k} \quad (2.2)$$

where

- $\bar{\xi}_{2D}$ = 2-D vorticity vector (s^{-1});
- \hat{k} = unit vector in the z -direction;
- u = x -component of velocity (m/s);
- v = y -component of velocity (m/s);
- x = downstream (longitudinal) direction of flow (m); and
- y = cross-stream (latitudinal) direction of flow (m).

This represents a particle's rotation around the z -axis. Counterclockwise rotation has a positive 2-D vorticity and clockwise rotation has a negative 2-D vorticity. In this analysis, 3-D vorticity is calculated for the entire flow field. Also, 2-D vorticity is estimated by isolating the z -component of the vorticity vector. This 2-D calculation is an approximation because the vorticity is still calculated from the 3-D velocity vector, not from the depth-averaged velocity.

2.7 Reach Extents

The analyses in this thesis concerned only the pool habitat in the WWP reaches and natural reaches. In order to concentrate on the pools, smaller analysis reaches were isolated from the larger hydraulic models. Each of these reaches was the same length (20 m) and the mean area

was 185 m² at low flow ($\sigma = 35 \text{ m}^2$), 238 m² at medium flow ($\sigma = 30 \text{ m}^2$), and 278 m² at high flow ($\sigma = 35 \text{ m}^2$). Each reach started at the top of the pool and ended near the bottom of the same pool. In the WWP, the top of the pool was clearly at the drop structure. In the natural reaches, the top of the pool was determined by examining the modeled reaches for areas of rapidly increasing depth. There were three WWP pools, denoted as WWP1, WWP2, and WWP3 (from downstream to upstream). In the natural reach, there were four pools, denoted as NR1-A, NR1-B, NR2, and NR3 (from downstream to upstream) (Figure 2.1).

As stated earlier, the high-velocity flow over the drop structure was not included in the post-process analysis performed in this study. Clearly, this flow (which had velocity as high as 4 m/s in some reaches) is the primary influence on the downstream hydraulic characteristics, so it was of course included in the models and great care was taken to model it accurately. The reader is encouraged to follow the work of Fox [in prep] for a full description of the flow characteristics found over the drop structure and their influence on fish passage.

2.8 2-D Habitat Modeling

The habitat suitability equations used in this thesis were developed by Miller Ecological Consultants, Inc. using data collected by CPW [Miller and Swaim, 2011]. Ideally, habitat suitability criteria would be developed for the specific river of interest, but none were available for the St. Vrain. Fortunately, criteria were available from the Cache la Poudre River, a similar adjacent watershed. The Cache la Poudre River drains a 4,895-km² watershed on the eastern slope of the Rocky Mountains, approximately 50 km north of the St. Vrain. The river has a similar flow regime, geomorphic context, and fish species assemblage to the St. Vrain, though it is larger, with high flows ranging from 85 to 140 cms. Due to the similarities, it was assumed that fish habitat use in the two rivers is also similar. The species and life stages analyzed in this

study are juvenile and adult rainbow trout, juvenile and adult brown trout, longnose dace, and longnose sucker. 'Adults' were classified as having lengths greater than 150 mm. The hydraulic input for each of the species-specific habitat suitability equations developed by Miller and Swain [2011] includes depth and depth-averaged velocity, and the output was an HSI value ranging between 0 (no habitat value) and 1 (optimal habitat). Each equation had upper limits for depth and velocity inputs. Any computational cell with a depth or velocity exceeding these limits was assigned an HSI value of 0. Any computation cell with an HSI value greater than 1, but with depth and velocity parameters within the pre-defined limits, was assigned a value of 1. HSI calculations were performed on the hydraulic output data from FLOW-3D using R statistical computing software [R Development Core Team, 2012]. Contour plots showing habitat quality were developed for each reach. Any areas with an HSI value greater than 0 were deemed to have 'some' habitat, while areas with an HSI value greater than 0.5 were classified as 'good' habitat, following Miller [2013].

To compare habitat quality in WWP reaches and natural reaches, a Student's *t*-test and Wilcoxon signed-rank test were used. Neither test is ideal for these data, since a *t*-test assumes a normal distribution and the Wilcoxon test has low statistical power with small sample sizes. However, considered together, they can provide more-meaningful results for small, potentially non-normal samples than if either were used alone [Hess, 2013]. For this analysis, a result was considered significant only when *both* tests produced a *p*-value less than 0.05.

CHAPTER 3 RESULTS

3.1 2-D and 3-D Hydraulic Variables

The modeled hydraulic conditions of the WWP pools were substantially different than the conditions in the natural pools. Also, a 2-D interpretation of hydraulic results painted a different picture of flow conditions than a 3-D interpretation.

3.1.1 Depth

Model results showed the maximum depth in the WWP pools (averaged for all WWP pools) was higher than the maximum depth in the natural pools (averaged for all natural pools) for all flow rates (Table 3.1). To show an example of the differences in depth in a visual manner, two representative pools were chosen, one WWP pool (WWP2) and one natural pool (NR3) (Figure 3.1). WWP2 was chosen because it had the most rapid and complex flow of any of the WWP pools (determined by a visual comparison of the pools), while NR3 was chosen because it was the deepest of the natural pools and provided the best comparison to the deeper WWP pools. These same pools are used to compare other hydraulic variables below, and the medium flow rate (4.25 cms) was always used. In all color and gray-scale contour plots, flow is from left to right, in the positive x -direction.

Table 3.1. Maximum flow depth (m) in WWP pools and natural pools at all flow rates.

Flow Rate	WWP Pools	Natural Pools
Low	1.5	0.6
Medium	1.8	0.9
High	2.1	1.1

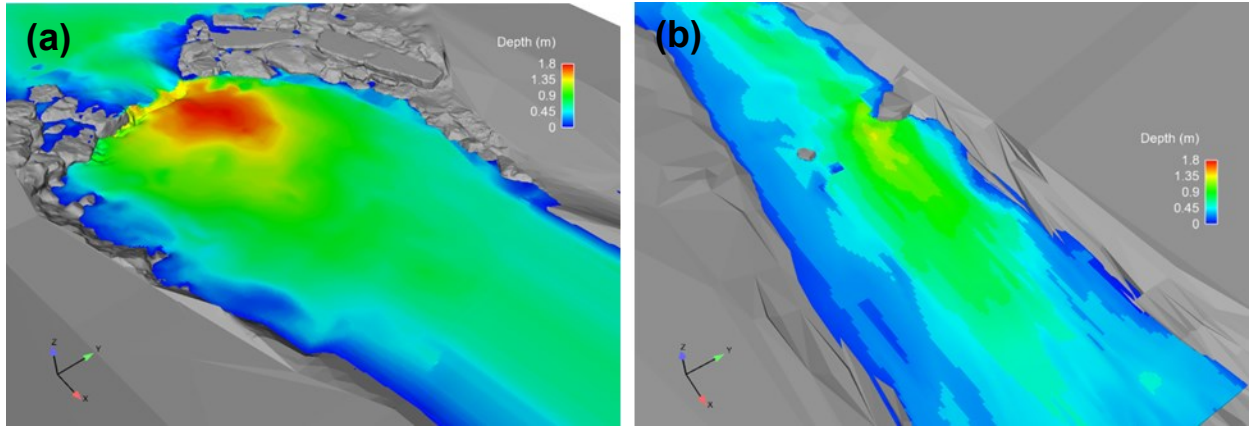


Figure 3.1. Flow depth (m) in pools: (a) WWP2 and (b) NR3 at 4.25 cms. The pool in the natural reach starts just below the protruding boulder on the left bank.

3.1.2 Velocity

The maximum depth-averaged velocity was greater in the WWP pools than in the natural pools for all flow rates (Table 3.2). Depth-averaged velocity for the two representative pools, WWP2 and NR3, is shown in Figure 3.2. The depth-averaged velocity in the thalweg in WWP2 was approximately 2.0 m/s, and the depth-averaged velocity in the thalweg in NR3 was approximately 1.9 m/s.

Table 3.2. Maximum depth-averaged velocity (m/s) in WWP pools and natural pools at all flow rates.

Flow Rate	WWP Pools	Natural Pools
Low	2.3	0.8
Medium	3.6	2.1
High	3.8	2.6

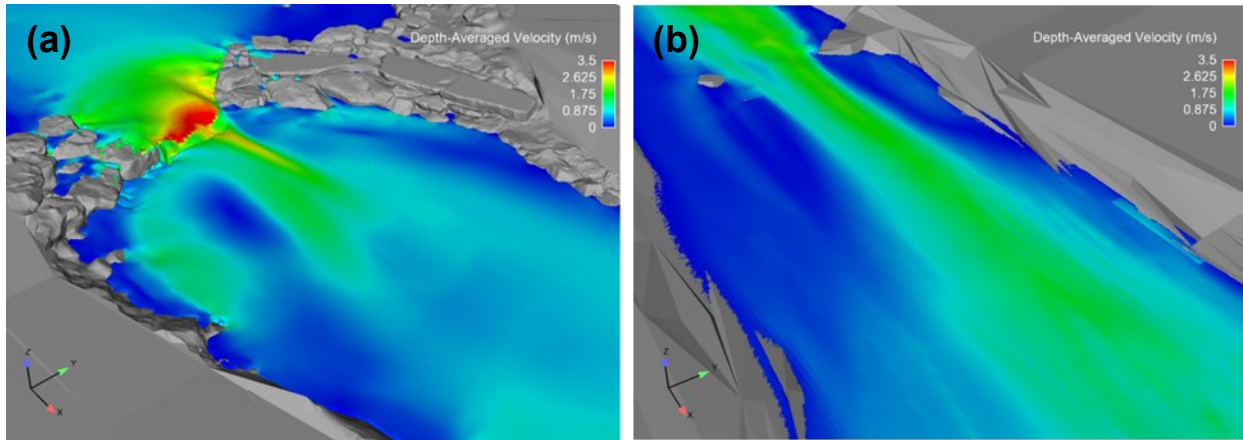


Figure 3.2. Depth-averaged velocity (m/s) in pools: (a) WWP2 and (b) NR3 at 4.25 cms.

Cross-sections were sampled in these two representative pools to better understand the 3-D velocity distribution. A cross-section sampled at the top end of the pool in NR3 showed a typical open-channel velocity profile, with lower velocities near the channel bed, and higher velocities near the surface (considering only the downstream velocity component) (Figure 3.3b). The vertical velocity component in this cross-section was negligible. Conversely, a cross-section sampled just below the drop structure in WWP2 included a submerged jet and produced a velocity profile that was much higher near the bed than at the surface (Figure 3.3a). There was also a substantial vertical velocity component in this cross-section, where downward and upward flows reached 1 m/s.

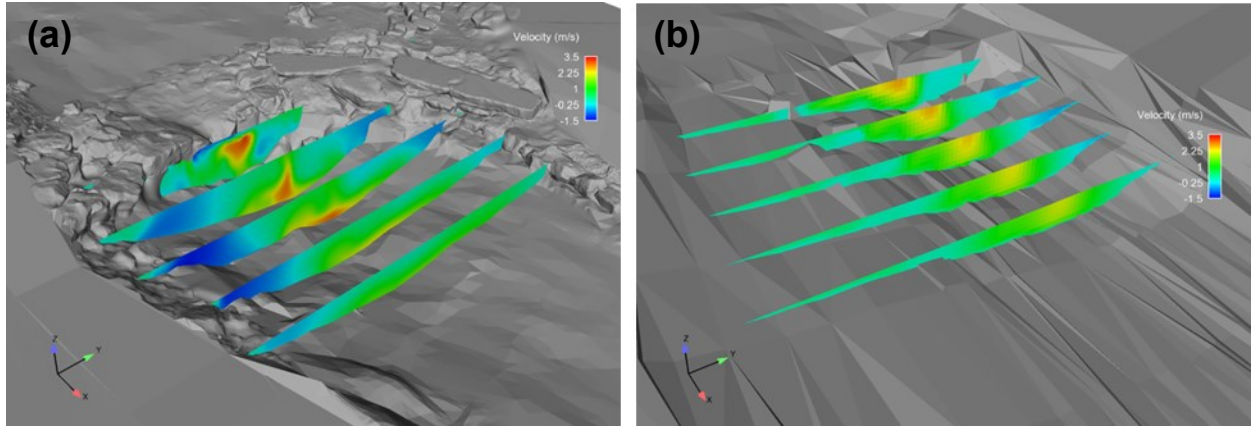


Figure 3.3. Cross-sections showing the downstream velocity component (m/s) in pools: (a) WWP2 and (b) NR3 at 4.25 cms.

3.1.3 TKE

The maximum turbulent kinetic energy (TKE) values for each flow rate were averaged for all the WWP pools and all the natural pools. TKE was consistently higher in the WWP pools than the natural pools, and increased with flow rate (Table 3.3). The two representative pools, WWP2 and NR3, are shown in Figure 3.4. The cross-sections in the natural pool show that areas with high turbulence were concentrated in the upper half of the water column in the thalweg, while the cross-sections in the WWP pool show that areas of high turbulence were not confined to the thalweg and extended laterally across the pools.

Table 3.3. Maximum TKE (m^2/s^2) in WWP pools and natural pools for all flow rates.

Flow Rate	WWP Pools	Natural Pools
Low	0.19	0.03
Medium	0.40	0.17
High	0.51	0.21

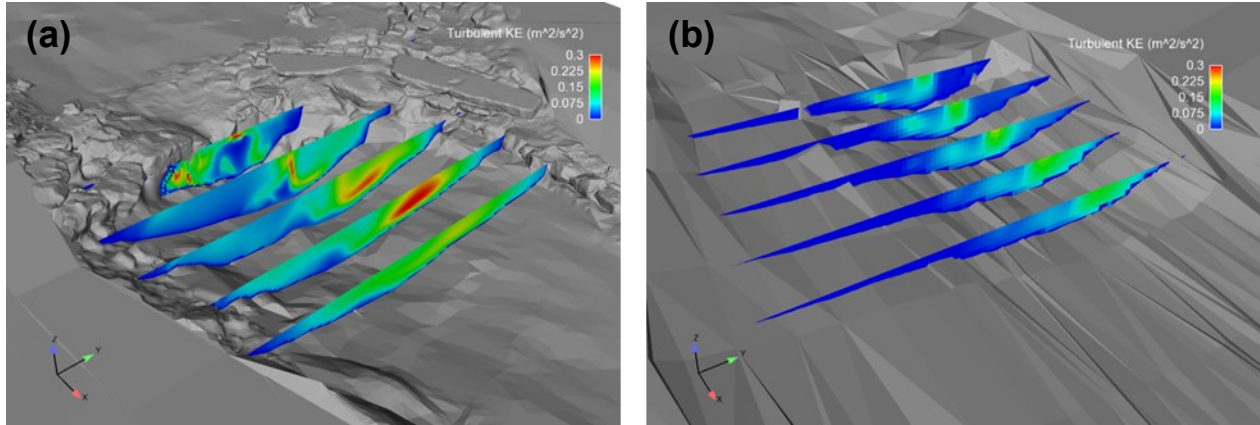


Figure 3.4. Cross-sections showing TKE (m^2/s^2) in pools: (a) WWP2 and (b) NR3 at 4.25 cms.

3.1.4 Vorticity

The maximum 3-D and 2-D vorticity values for each flow rate were averaged for all the WWP pools and all the natural pools (Table 3.4). Both vorticity metrics were consistently higher in the WWP pools than the natural pools. Neither metric had a consistent relationship with flow rate. Three-dimensional vorticity in the two representative pools, WWP2 and NR3, is shown in Figure 3.5. The cross-sections in the WWP pool show larger spatial distribution of higher vorticity magnitudes than the natural pool. In the NR3 pool, higher vorticity values were concentrated near the bed, as expected due to higher shear stress in that area. In the WWP2 pool, high vorticity was distributed unevenly through the pool and throughout the water column. The areas of high shear stress, which cause high vorticity, were found near the bed and within jets and eddies.

Table 3.4. Maximum (a) 3-D and (b) 2-D vorticity (s^{-1}) in WWP pools and natural pools for all flow rates.

(a) maximum 3-D vorticity in all pools (s^{-1})		
Flow Rate	WWP Pools	Natural Pools
Low	9.3	4.5
Medium	17.7	10.8
High	17.7	8.3

(b) maximum 2-D vorticity in all pools (s^{-1})		
Flow Rate	WWP Pools	Natural Pools
Low	5.7	2.0
Medium	12.0	4.5
High	10.3	5.5

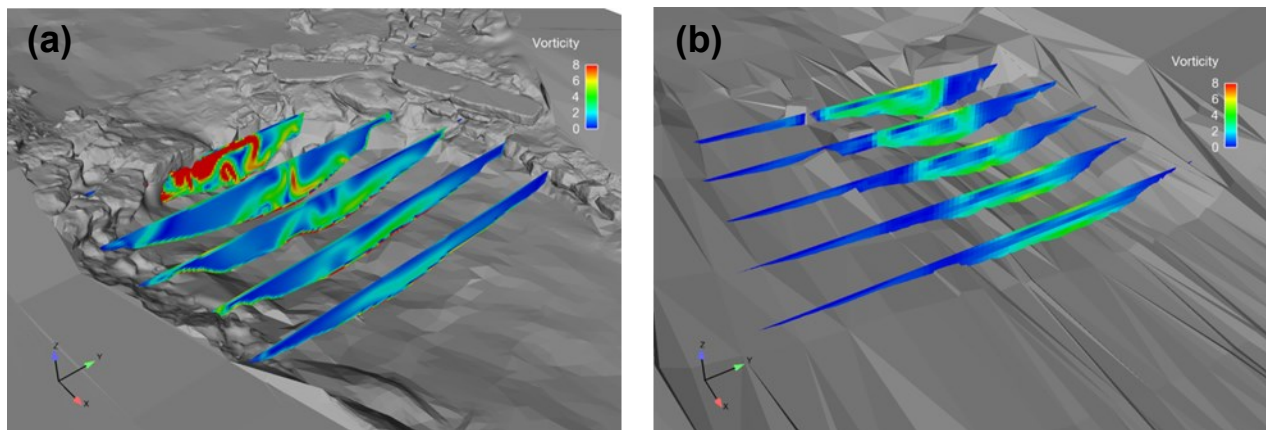


Figure 3.5. Cross-sections showing 3-D vorticity (s^{-1}) in pools: (a) WWP2 and (b) NR3 at 4.25 cms.

There were clear differences between 2-D and 3-D vorticity, and these were examined further by extracting horizontal slices of flow in the WWP2 rendering. At a slice just below the water surface, there was a large eddy on the right-side of the channel (Figure 3.6). The plot of 3-D vorticity shows a wide swath of high vorticity in this region, indicating an area of tumbling complex flow. In the 2-D rendering, the vorticity in and around that eddy was almost completely damped out, meaning that most of the vorticity in that area was not in the horizontal plane. At the deepest slice, 0.6 m below the water surface, both the 2-D and 3-D renderings captured the high

levels of vorticity in the center jet, but the 2-D rendering did not show the large area of higher vorticity downstream of that jet (Figure 3.7). From field surveys, it was clear that this downstream area contained flow complexity in the form of churning and boils, and that information is lost in the 2-D interpretation. Just above the channel bed at 1.2 m below the water surface, the vorticity magnitudes were twice as high in the 3-D rendering as in the 2-D rendering (Figure 3.8). The tumbling caused by shear stresses near the bed was resolved in 3-D, but not in 2-D.

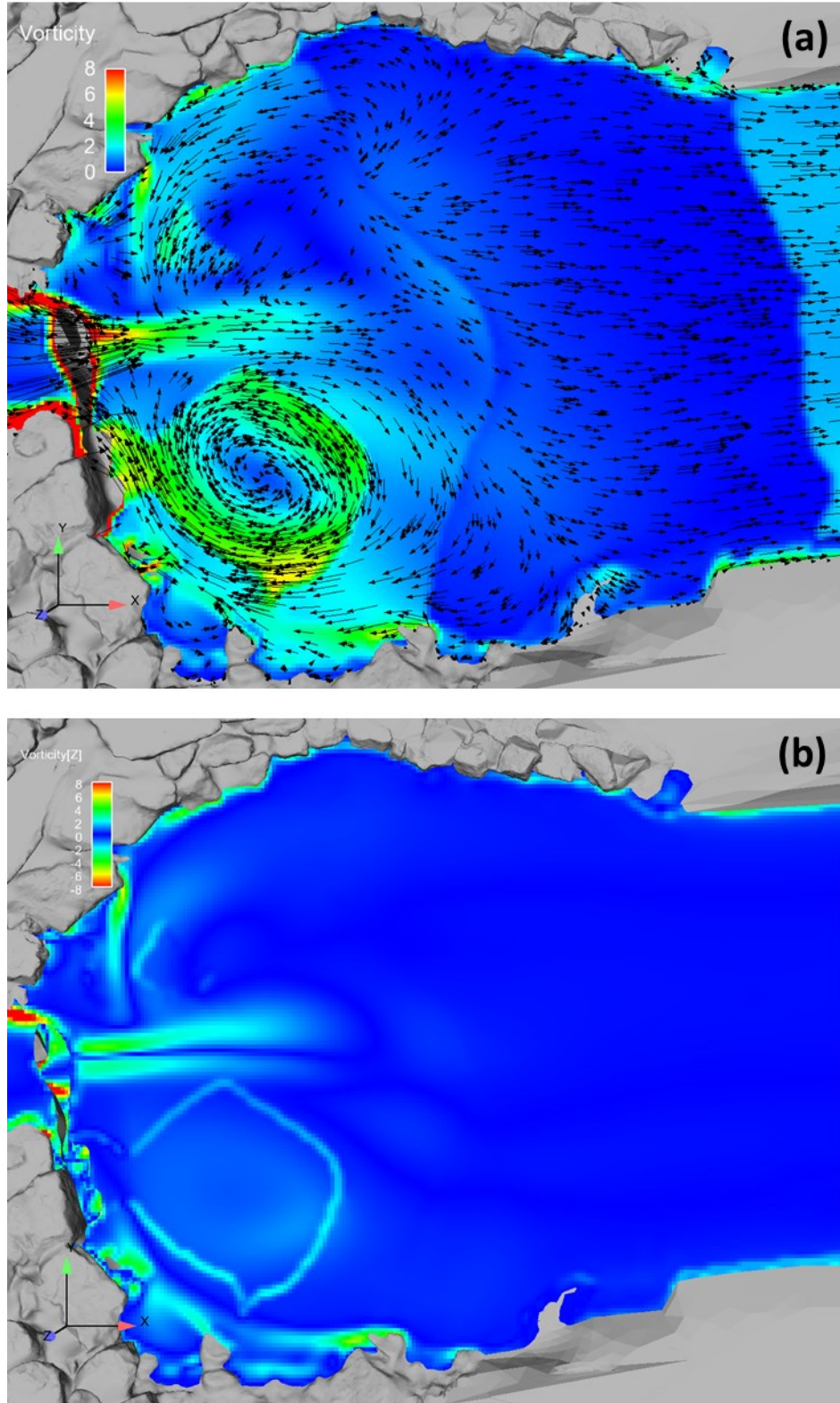


Figure 3.6. Plan view of WWP2 pool just below water surface at 4.25 cms: (a) color contours represent 3-D vorticity values (s^{-1}) and arrows represent direction of flow in the horizontal (XY) plane, and (b) color contours represent absolute value of 2-D vorticity values (s^{-1}).

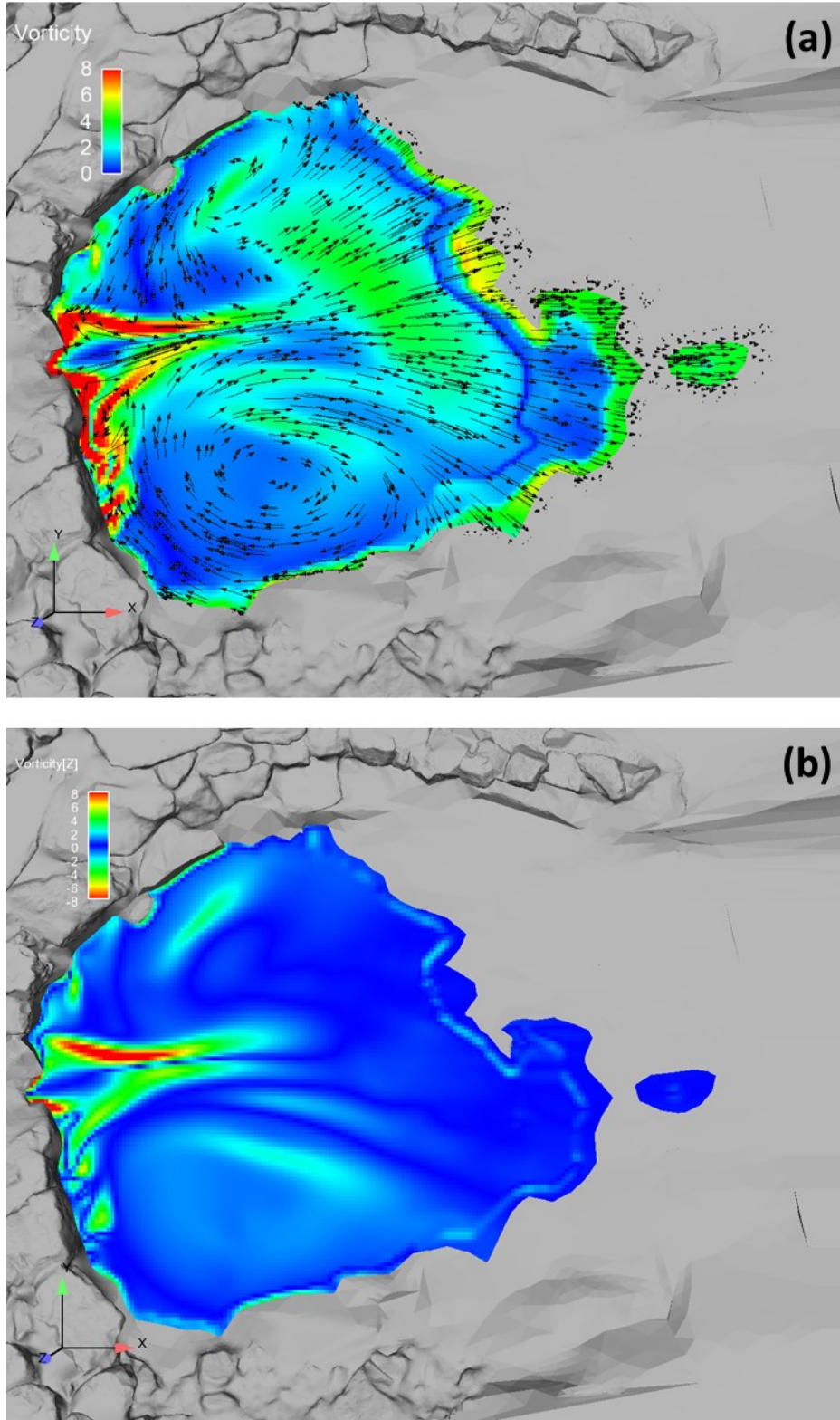


Figure 3.7. Plan view of WWP2 pool 0.6 m below water surface at 4.25 cms: (a) color contours represent 3-D vorticity values (s^{-1}) and arrows represent direction of flow in the horizontal (XY) plane, and (b) color contours represent absolute value of 2-D vorticity values (s^{-1}).

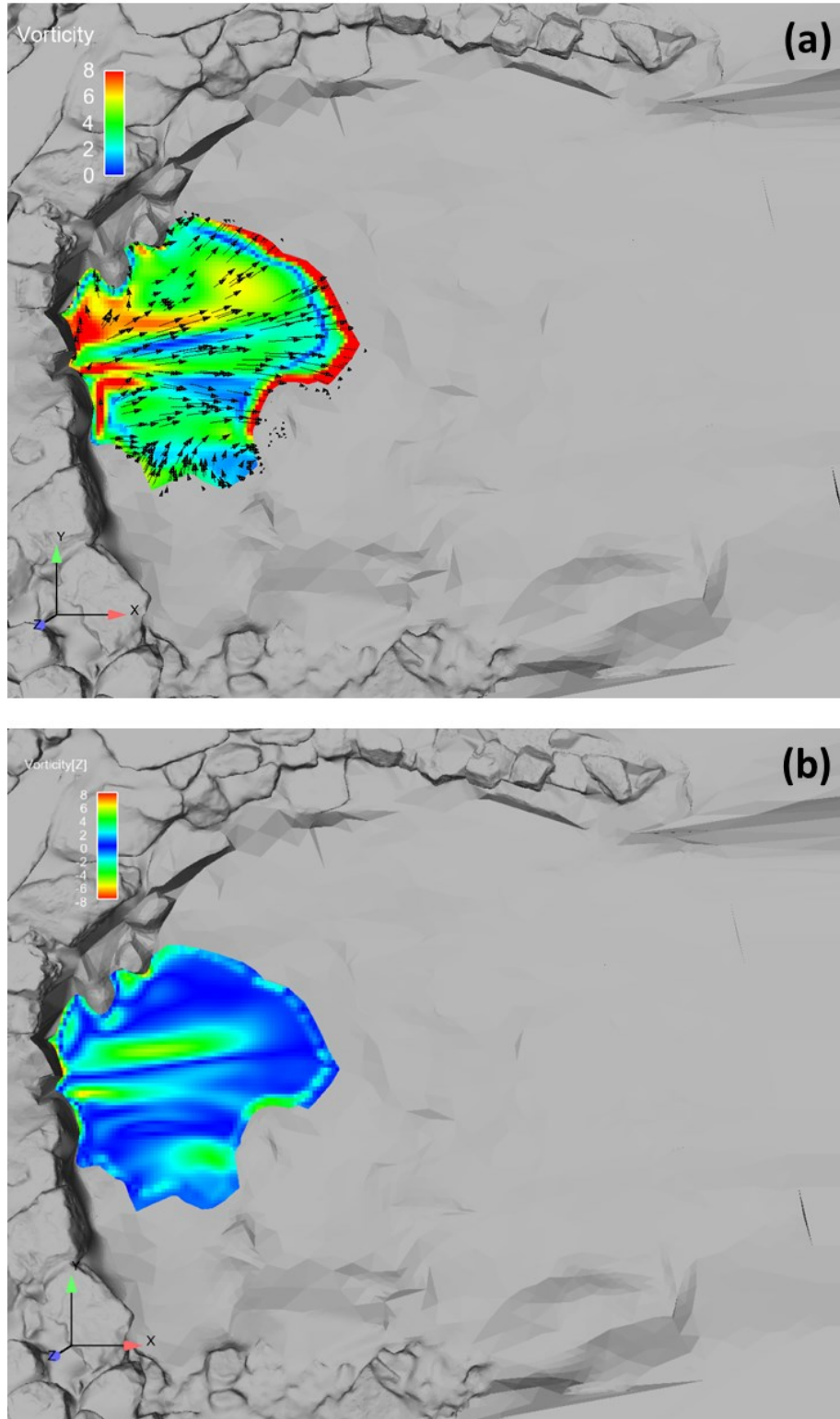


Figure 3.8. Plan view of WWP2 pool 1.2 m below water surface and just above channel bed at 4.25 cms: (a) color contours represent 3-D vorticity values (s^{-1}) and arrows represent direction of flow in the horizontal (XY) plane, and (b) color contours represent absolute value of 2-D vorticity values (s^{-1}).

3.2 3-D Flow Patterns

Flow patterns in the WWP reaches included large lateral and vertical eddies just below the drop structure. In the natural reaches, flow was primarily in the downstream direction, with very little recirculation. Figure 3.9 shows an example of the differences in flow patterns based on the representative reaches, WWP2 and NR3.

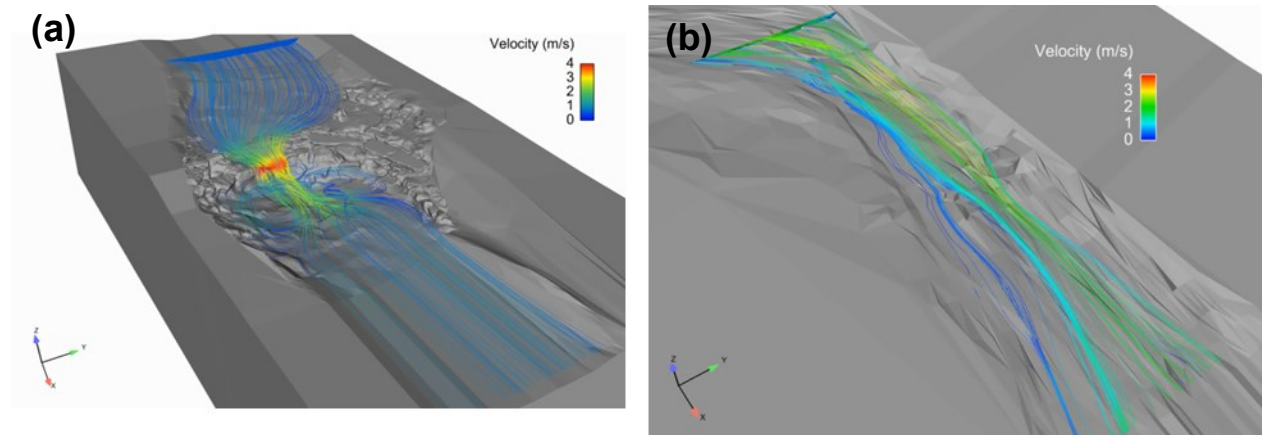


Figure 3.9. Streamlines showing patterns of flow in pools: (a) WWP2 and (b) NR3 at 4.25 cms. Coloring represents velocity magnitude (m/s).

3.3 2-D Habitat Modeling

The 2-D habitat analysis resulted in few significant differences between the predicted habitat for WWP pools and natural pools. The depth limits for the habitat suitability criteria were exceeded in small areas of the WWP pools for native longnose dace and longnose sucker at all flow rates. Maximum depth-averaged velocity in small areas of the WWP pools exceeded the criteria limits for all species and all flow rates, while the maximum depth-averaged velocity in small areas of the natural pools exceeded criteria limits for all species at medium and high flow rates.

Percentage of pool area with good habitat for each species life stage and flow rate are reported in Table 3.5.

Table 3.5. Percentage of pool area with good habitat (HSI > 0.5) for each species life stage and flow rate. Grey highlight indicates significant differences between WWP pools and natural pools ($p < 0.05$ for Wilcoxon and t -test).

Flow (cms)	Juvenile Brown		Adult Brown		Juvenile Rainbow		Adult Rainbow		Dace		Sucker	
	WWP	Natural	WWP	Natural	WWP	Natural	WWP	Natural	WWP	Natural	WWP	Natural
	0.42	14.1	16.3	0.3	0.2	37.5	19.6	3.6	0.8	5.2	25.5	21.8
4.25	9.6	8.6	8.8	0.9	18.7	15.3	17.6	0.7	40.7	15.3	42.0	42.8
8.5	7.7	8.6	6.2	0.9	13.0	11.5	16.7	0.7	21.6	14.0	20.3	28.0

3.3.1 Juvenile Brown Trout

Modeled juvenile brown trout habitat was concentrated around the margins of the WWP pools and decreased as the flow rate increased. At low flow in the natural pools, habitat was concentrated in the thalweg, but moved to the margins of the channel as flow increased. When the average percentage of good habitat ($HSI > 0.5$) was compared between WWP pools and natural pools, there were no significant differences (Table 3.5).

3.3.2 Adult Brown Trout

There was very little adult brown trout habitat in WWP pools at any flow rate. The small areas of good habitat were concentrated at the margins of eddies and jets (Figure 3.10). The amount of habitat increased slightly with flow rate. Good habitat was minimal in the natural pools and did not change with flow rate. At low and high flow rates, there were no significant differences between the percentage of good adult brown trout habitat in the WWP pools and natural pools (Table 3.5). At medium flow rate, the WWP pools had significantly higher good habitat (8.8%) than the natural pools (0.9%) (t -test $p = 0.001$; Wilcoxon $p = 0.049$) (Figure 3.11).

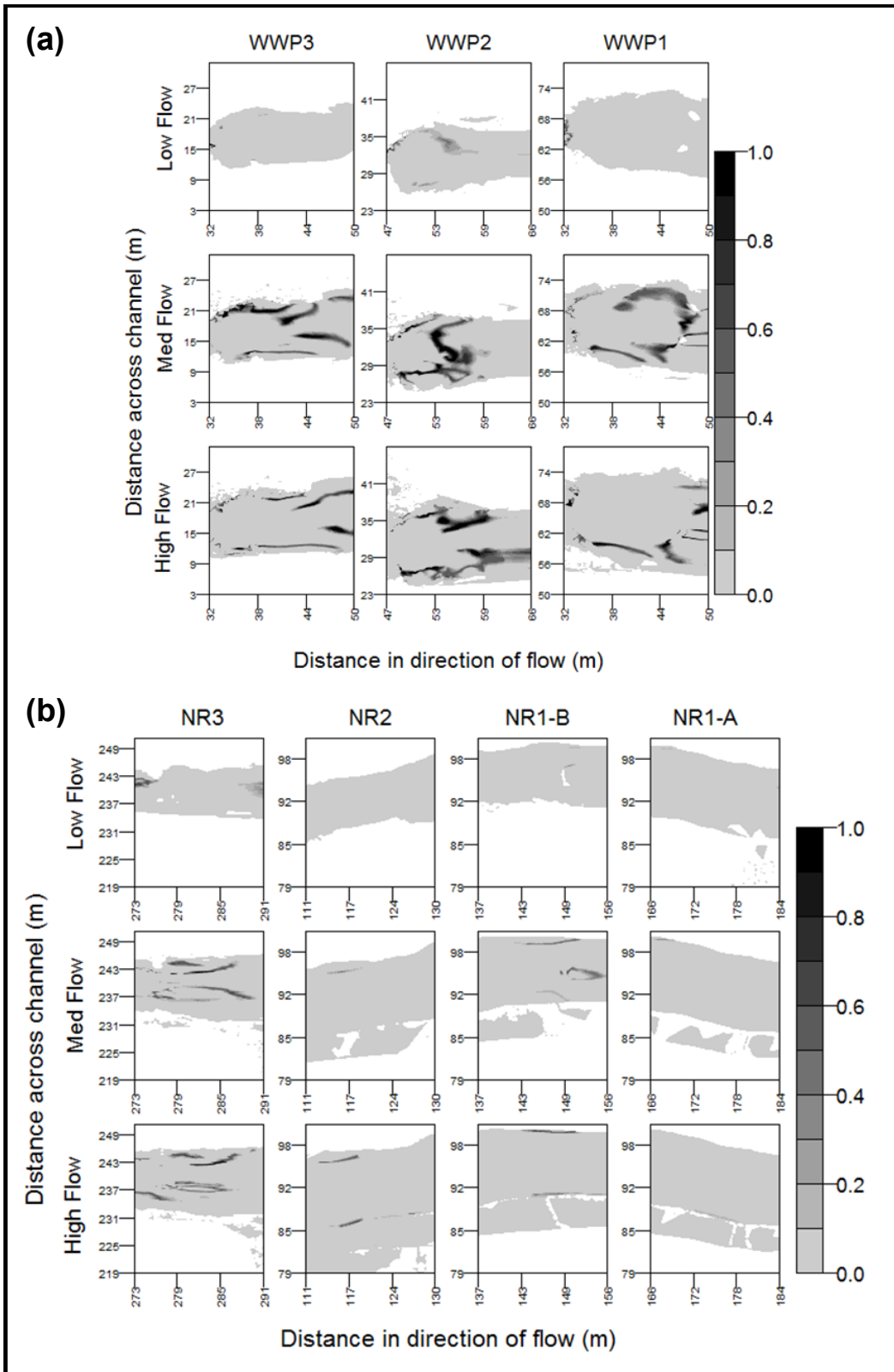


Figure 3.10. Habitat suitability results for adult brown trout in: (a) WWP pools and (b) natural pools.

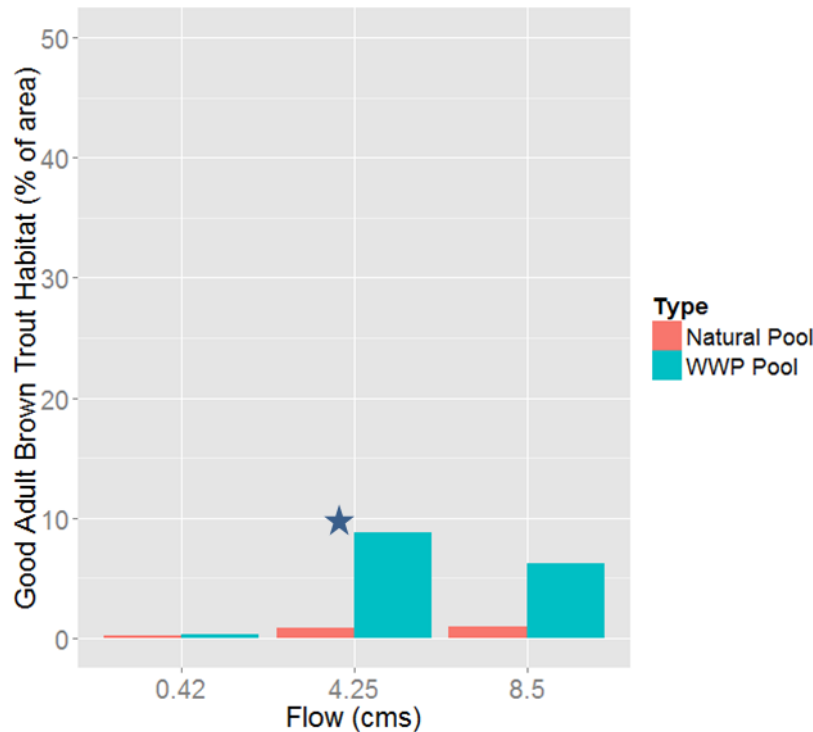


Figure 3.11. Average good adult brown trout habitat as a percentage of wetted area for low, medium, and high flow rates. Stars indicate significant differences in amount of habitat between WWP pools and natural pools.

3.3.3 Juvenile Rainbow Trout

The 2-D habitat analysis showed that juvenile rainbow trout habitat was high in the WWP pools and found everywhere except for the deepest parts of the pools. The amount of good habitat decreased as the flow rate increased, but remained above 13% of area. At low flow in the natural reaches, juvenile rainbow trout habitat was concentrated in the thalweg, but moved to the margins of flow as flow rate increased. There were no significant differences between percentage of good habitat in WWP pools and natural pools (Table 3.5).

3.3.4 Adult Rainbow Trout

In the WWP pools, adult rainbow trout habitat was concentrated in areas of higher depth, but as flow rate increased, habitat moved to the margins of jets and eddies, similar to adult brown

trout habitat (Figure 3.12). The amount of habitat in the WWP pools generally increased with flow rate. There was minimal habitat available in the natural pools, and changes among flow rates were not apparent. For medium flow, the percentage of good habitat was significantly higher in the WWP pools (17.6%) compared with natural pools (0.7%) (*t*-test $p = 0.00002$; Wilcoxon $p = 0.043$). The same was true for high flow where WWP pools had an average of 16.7% good habitat and natural pools had an average of 0.7% good habitat (*t*-test $p = 0.008$; Wilcoxon $p = 0.049$) (Table 3.5; Figure 3.13).

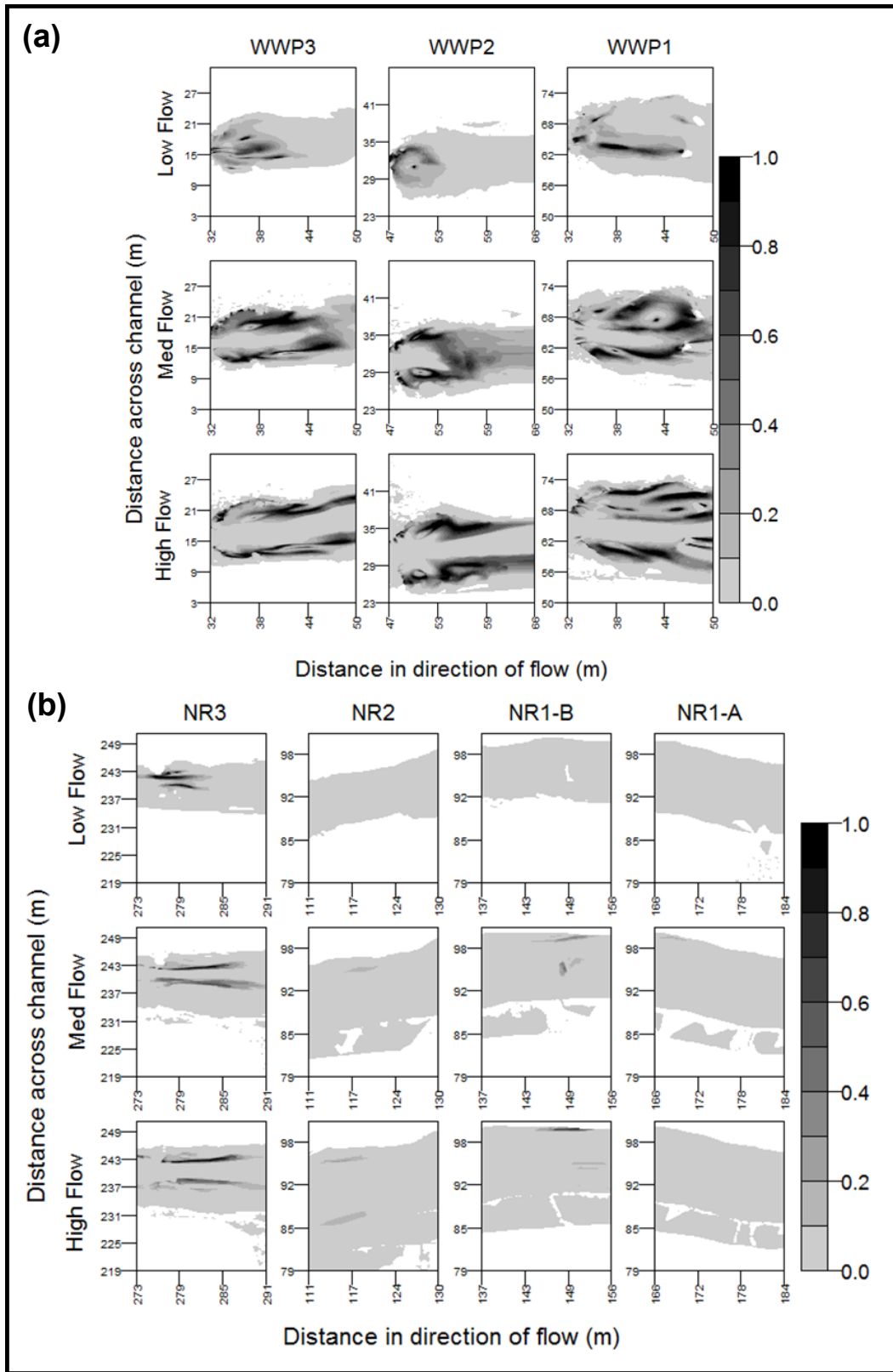


Figure 3.12. Habitat suitability results for adult rainbow trout in: (a) WWP pools and (b) natural pools.

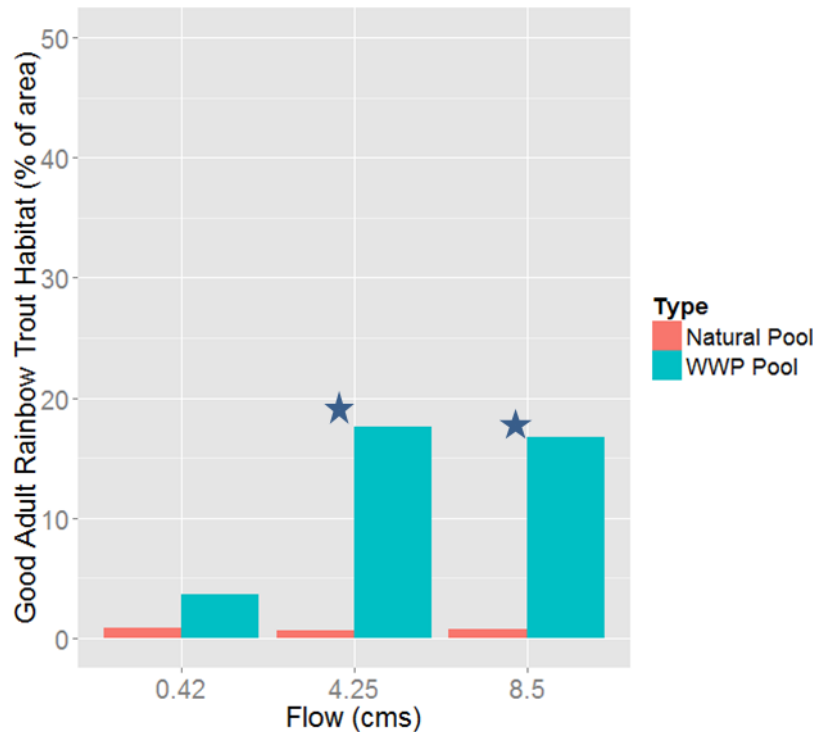


Figure 3.13. Average good adult rainbow trout habitat as a percentage of wetted area for low, medium, and high flow rates. Stars indicate significant differences in amount of habitat between WWP pools and natural pools.

3.3.5 Longnose Dace

Predicted longnose dace habitat was abundant in the WWP pools, and occurred everywhere except for in the deepest part of the pools. The total amount of habitat decreased as flow increased, but the amount of good habitat was greatest at medium flow. In the natural pools, habitat was concentrated in the thalweg for low flow, and then moved to the margins as flow rate increased. Longnose dace was the only species that had a higher percentage of good habitat in the natural pools than in the WWP pools, though this was only true at low flow and was statistically significant for only one test (t -test $p = 0.002$; Wilcoxon $p = 0.057$) (Table 3.5). At medium flow, there was a higher percentage of good habitat in the WWP pools than in the natural pools at medium flows, but again, this was only statistically significant for one test (t -test $p = 0.04$; Wilcoxon $p = 0.057$).

3.3.6 *Longnose Sucker*

Predicted longnose sucker habitat occurred throughout the WWP pools and natural pools, except in the deepest pools at the highest flows. There were no significant differences in longnose sucker habitat between WWP pools and natural pools (Table 3.5).

CHAPTER 4 CASE STUDY: BIOMASS SURVEYS

CPW has an ongoing study to quantify biomass of introduced and native fishes in the North St. Vrain. They are surveying fish biomass in the same reaches and pools described in this thesis. Beginning in Fall 2010, electroshocking surveys occurred each fall (in October or November) and spring (in April). Fall surveys were conducted during low flow and timed to coincide with brown trout spawning, while spring surveys corresponded with rainbow trout spawning. Spring and fall surveys occurred well before and after the summer period of heavy recreational use in the river.

Surveys were conducted with four hand-held electrodes connected to a truck-mounted generator. Surveyors used a standard three-pass depletion method to estimate the number of fish in each reach. Each fish caught was identified to species, measured, weighed, passive integrated transponder (PIT) tagged (if not already tagged), and released in the same pool where it was captured. The four species captured in the pools were rainbow trout, brown trout, longnose dace, and longnose sucker.

The results of the Fall 2010 and Fall 2012 biomass surveys for adult brown trout (the most abundant fish species at the site) are shown below. The 2011 results are not presented because they were affected by unusually prolonged high flow rates that potentially confounded the field surveys. High flow makes electroshocking difficult due to low-water conductance, and because deep fast-moving water makes it difficult to physically catch the fish that are successfully shocked. The capture probability in each pass during 2011 was insufficient for reliable population estimates [Kondratieff, 2013]. The Fall 2010 surveys followed a high flow year as well, but peak flow was short and did not extend into the fall. Fall 2012 surveys occurred after a period of spring and summer drought.

When normalized by pool surface area, adult brown trout biomass was not significantly different in natural pools and WWP pools for either year (Figure 4.1c). However, when biomass was normalized by pool volume, biomass averages were significantly higher in the natural pools than the WWP pools for both years (Figure 4.2c). The per volume analysis accounts for the fact that the WWP pools are much deeper than the natural pools and, therefore, provide much more physical space for fish to inhabit.

The initial results of these biomass surveys caused concern among local fish biologists, and provided an impetus for further studies, including the modeling study presented in this thesis. Continuation and further analysis of the biomass surveys will be completed by CPW researchers and will be presented in a forthcoming publication.

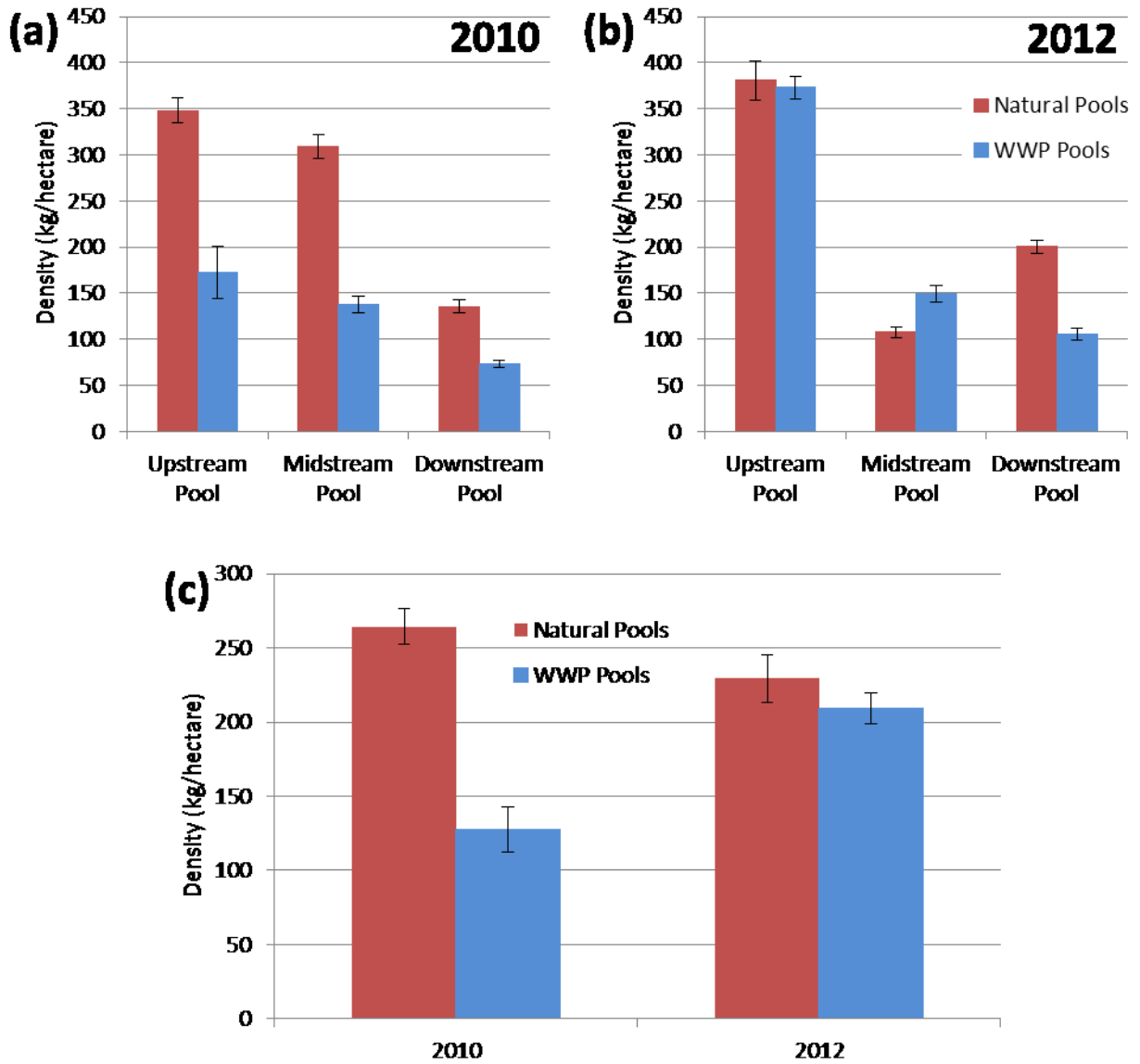


Figure 4.1. Adult brown trout biomass normalized by pool surface area: (a) biomass in each pool in 2010, (b) biomass in each pool in 2012, and (c) average biomass in WWP pools and natural pools in 2010 and 2012. Error bars represent 95% confidence intervals.

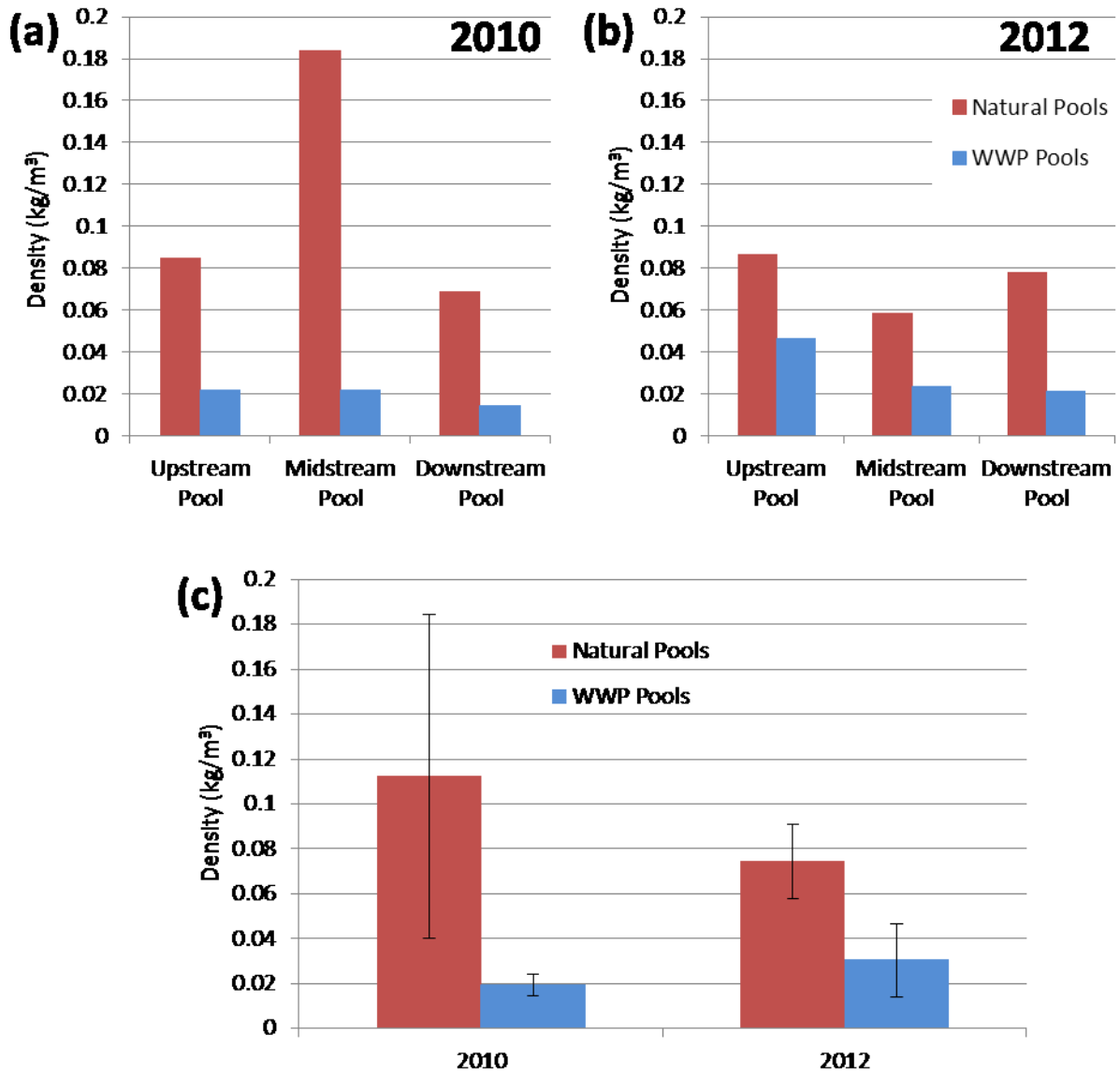


Figure 4.2. Adult brown trout biomass normalized by pool volume: (a) biomass in each pool in 2010, (b) biomass in each pool in 2012, and (c) average biomass in WWP pools and natural pools in 2010 and 2012. Error bars represent 95% confidence intervals.

CHAPTER 5 DISCUSSION

5.1 Hydraulic Variables

Substantial differences were found between the hydraulic characteristics in WWP pools and natural pools. Depth, depth-averaged velocity, TKE, and 2-D and 3-D vorticity all had higher magnitudes in the WWP pools than in the natural pools. Pairing these results with the CPW biomass study results, which showed higher biomass per volume in the natural pools than the WWP pools, suggests that correlations could exist between these hydraulic variables and biomass. Correlations are especially important to consider for variables that have not quantitatively been linked to habitat quality thus far, specifically TKE, 2-D vorticity, and 3-D vorticity. All three of these metrics are substantially higher in the WWP pools than the natural pools, while biomass per volume is higher in the natural pools, which could provide a starting point for examining the effects of these flow characteristics on habitat quality in the future.

In the comparison between 2-D and 3-D methods, velocity and vorticity showed stark differences between the two methods, and TKE provided information that was unavailable with 2-D methods. Velocity is a fairly straightforward hydraulic variable to calculate in 2-D and 3-D. The effects of velocity on aquatic habitat are also fairly well-understood compared to the other variables, and studies have related fish swimming abilities and resting preferences to velocity magnitudes for use in HSI calculations [Bovee *et al.*, 1998]; however, it is still common practice to use depth-averaged velocity for these determinations. In a channel or river with very little complexity, depth-averaged velocity is a useful metric because the logarithmic velocity profile is very predictable. The expected velocity profile can be seen in NR3 (Figure 3.3b), where there is slower velocity near the bed and faster velocity near the surface. Due to the drop structure and the submerged jet, the velocity distribution in WWP2 is exactly the opposite, with faster velocity

near the bottom of the water column and slower velocity on the surface. It is clear from a 3-D rendering that these two flow conditions are very different, but the contour plot of depth-averaged velocity in WWP2 and NR3 shows almost identical magnitudes through each pool (Figure 3.2). The depth-averaged velocity in the thalweg 2 m downstream of the top of the pool is 1.9 m/s in the WWP reach and 1.8 m/s in the natural reach. If the depth-averaged information was the only data available, one could erroneously assume that flow conditions were functionally the same and know nothing about the actual distribution of velocity beneath the water surface.

It is important to consider what conditions fish in this river are accustomed to, which in the case of velocity, likely include slower near-bed flows. A fish could be accustomed to sheltering itself in the bottoms of pools that provide ample cover and adequately low velocities, but will not be prepared for the high-velocity conditions at the bottom of a deep WWP pool. Bremset [2000] studied brown trout in Norwegian rivers and found that they preferred to be about 80 cm above the channel bed in late summer, likely because the food sources in that region were plentiful and they could outcompete other fishes for this prime feeding location. In late fall, when food sources declined, they would move lower in the water column and spend more time near the channel bed. If similar behavior occurs in the St. Vrain WWP, it could mean that smaller fish that are pushed out of the prime mid-depth feeding area would encounter intolerable near-bed velocities and be forced to find another pool. Also, moving to the bottom of the water column in late fall would not be a viable option for fish, since lower temperatures and decreased food availability in winter would make it more difficult for trout to rest and swim in higher near-bed velocities.

In a natural step-pool system, which would be found in streams with a higher gradient than the St Vrain, fish might be more accustomed to the high velocities and complex flow patterns found in WWPs. Very similar flow patterns are found in step pools created by lateral

constrictions, including plunging flow, hydraulic jumps, and recirculating eddies [Thompson *et al.*, 1998]. However, large lateral constrictions are not found naturally in this section of the St. Vrain, and there is reason to believe fish would not be accustomed to this kind of flow complexity.

The spatial distribution of high vorticity varied greatly between the two representative pools, WWP2 and NR3 (Figure 3.5). In the natural pool, vorticity was concentrated near the thalweg, and again it can be assumed that fish in this region are accustomed to this pattern of vorticity distribution. In the WWP, the areas of maximum vorticity were much larger, and were spread laterally across most of the pool. High vorticity was not confined to just the near-bed and near-surface areas; instead, it was distributed unevenly through the water column. Vorticity is correlated with flow complexity, and exact values regarding fish preference are not known. It is possible that low levels of vorticity are tolerable and possibly even preferable to many fish, whereas high levels, above a certain threshold, are no longer suitable.

Again, the role vorticity plays in determining optimal aquatic habitat is an open question, but if further research shows that high vorticity is detrimental or beneficial to certain fish, then vorticity must be characterized accurately. The results from this study show that resolving these characteristics in 3-D will be essential for prediction, supporting the results of a previous study that determined rotation in the vertical plane to be the best distinguishing factor between sampled modified and natural river reaches [Shields and Rigby, 2005]. In fact, highly realistic models will likely be needed to determine the relationships between vorticity and habitat quality.

The distribution of high TKE in the representative WWP pool (WWP2) is very different than the distribution in NR3 (Figure 3.4). High TKE values follow the location of the high-speed jet of water in the middle of the water column and extend laterally. If it is assumed that fish in this river are accustomed to the more natural conditions in NR3, it would mean that they expect a

jet of higher turbulence in the upper half of the water column along the thalweg, not a large region of submerged, high-magnitude TKE. Because of the approximations made in the turbulence modeling process within FLOW-3D, the values of TKE may not be absolutely correct when compared to other studies or measurements. However, these values do provide good relative measurements that allow comparison between WWP reaches and natural reaches as well as information about the spatial distribution of high turbulence. Turbulence can be beneficial or detrimental to fish, depending on the situation. Silva *et al.* [2012] found that fish in laboratory flumes tended to spend significantly less time in turbulent areas, presumably in an effort to conserve energy and maximize stability. However, the TKE magnitudes in their laboratory studies were much higher than the modeled magnitudes found in the St. Vrain WWP reaches or natural reaches. Small amounts of turbulence can attract fish and trigger migration as well as propel fish under the right conditions, but too much turbulence could prevent migration [Silva *et al.*, 2012]. Lacey *et al.* [2012] suggest that TKE not only influences fish directly through affecting swimming ability, but could also affect them indirectly through limiting food availability. This indirect affect could occur because food availability is influenced by local water velocity, which is often correlated with TKE. As certain amounts of turbulence and flow complexity are beneficial, it is probable that thresholds exist for turbulence effects and those thresholds could vary for different species, size classes, and hydraulic environments [Lacey *et al.*, 2012]. More research is necessary to determine what meaningful threshold values might be.

5.2 2-D Habitat Models

The 2-D HSI analysis for adult brown and rainbow trout suggests that there was significantly more good habitat in the WWP pools than the natural pools for medium flow (brown and rainbow) and high flow (only rainbow) based on depth and depth-averaged velocity.

For juvenile brown and rainbow trout, there were no significant differences between the WWP pools and natural pools. When these results are compared to the results from the CPW biomass study, an interesting contradiction emerges. The 2-D HSI results predict almost no good adult brown trout habitat in all of the natural reaches (Figure 3.10), but surveys found more than twice as much average adult brown trout biomass per volume in the natural pools than in the WWP pools (Figure 4.2c). Because the biomass data were collected at low flow, it would be expected that the 2-D HSI results at low flows would correspond with the biomass results; however, the HSI results show no significant difference between the predicted amount of good adult brown habitat in WWP pools and natural pools. From these data, it is difficult to extrapolate population estimates for brown trout at higher flows, but I can infer that the 2-D HSI results may not be a good predictor of actual biomass. Furthermore, in the WWP pools, the amount of predicted adult brown trout habitat was less than the amount predicted for any other species, which does not align with the fact that brown trout were by far the most abundant species in this stretch of river.

The lack of parallels between the 2-D HSI results and the biomass surveys could have many plausible explanations, and the truth likely lies in some combination of several factors. As explained above, HSI calculations are a gross simplification of a complex system; fish are living in a 3-D world while the habitat suitability criteria are based on 2-D parameters. The large differences between the 2-D and 3-D conditions pertaining to velocity, vorticity, and TKE were described above and are likely part of the explanation for the results of the biomass surveys. Also, the biomass surveys are a snapshot in time, but reflect the accumulated effects of antecedent flow conditions and biotic influences, whereas the 2-D HSI analysis reflects only hydraulic conditions at one model time step. Furthermore, fish habitat is not just affected by hydraulic conditions, but is also influenced by other physical factors such as substrate, bank complexity, and overhead cover, not to mention biological factors such as competition and

predation. The presence of kayakers or other recreational users in the WWP pools will also have an effect on the ways fish use pool habitat, and is in no way accounted for in habitat modeling. Overall, two-dimensional hydraulic modeling can be a useful way to describe habitat conditions, but until researchers can be sure that the hydraulic metrics used in the models accurately correlate to habitat quality in regions of very complex 3-D flow and within biologically complex systems, 2-D hydraulic modeling should not be used as the sole tool in habitat quality assessment.

5.3 Future Implications

Three-dimensional modeling has the potential to be a very important tool for the future of WWP design. As understanding of how 3-D hydraulic variables influence aquatic habitat suitability increases, design modifications can be tested to minimize any negative effects of those hydraulics. Rajaratnam and Katopidis [1997] studied the hydraulics of Denil fishways, a type of rectangular channel fish passage used at many impassible hydraulic structures such as dams. Specifically, they examined the resting pools between two linked Denil fishways to determine the configuration that provided the best actual rest for fish. These fishways are similar to WWPs because there is a high-velocity jet of water entering the top of the resting pools. To create an ideal environment for fish resting, they found it was important that there was enough water underneath the fishway so that the jet did not actually reach the fishway bed. A WWP could be designed based on this concept. The goal would be to augment the pool and the jet so that the high velocities did not reach the channel bed, but a desirable recreational wave was still created. Three-dimensional modeling would be ideal for this test because 2-D modeling would not capture the essential vertical flow component and field studies would be costly and labor intensive.

It is important to remember that this study represents one WWP in one river in Colorado, and cannot be used to make generalizations about the effects of WWPs on fish habitat in general, although it could inform future studies in parks with a similar size and geomorphic setting. Replications of the CFD process should be completed in other WWPs in order to understand general trends. Fish biomass studies should also be repeated in other parks, preferably with the inclusion of pre-construction baseline data.

Overall, it is clear that by ignoring the third dimension of flow in a 2-D hydrodynamic simulation, key information about hydraulic factors affecting habitat quality is being lost; however, 2-D modeling still has important utility. Two-dimensional modeling is substantially cheaper than 3-D modeling in terms of software cost (free 2-D software exists, while 3-D software is very expensive), computational power, required expertise, and time taken for data collection and modeling. The use of 2-D versus 3-D modeling must be assessed on a case-by-case basis. In the case of WWPs, this study suggests that 3-D modeling is the appropriate process. To make use of all the additional output provided by fully 3-D models, studies focused on the effects of 3-D flow metrics such as vorticity on aquatic habitat suitability must be carried out.

Finally, before management decisions are made, it is important to consider the overall effects of WWPs and determine if the benefits outweigh the costs. The issue of habitat quality in WWPs does not have any right or wrong answers, and even if WWPs potentially impact habitat quality in a negative manner, there are other ways habitat can be improved. WWPs can increase community awareness of rivers and improve people's connection with the environment, which in turn could lead to habitat enhancement projects in other sections of river.

CHAPTER 6 CONCLUSION

In this study, the effects of WWPs on aquatic habitat were examined using a 3-D hydrodynamic model. Two sections of a small river in Colorado were modeled for comparison: one relatively natural section, and one section containing a WWP with three engineered drop structures. All hydraulic metrics (depth, depth-averaged velocity, TKE, 2-D vorticity, and 3-D vorticity) had higher magnitudes in the WWP pools than in the natural pools. A 2-D habitat suitability analysis for juvenile and adult brown and rainbow trout, longnose dace, and longnose sucker predicted higher habitat quality in the WWPs than the natural reaches for adult brown and rainbow trout at some flow rates, while in-stream surveys showed higher fish biomass per volume in the natural pools. There are many other factors besides 2-D hydraulic variables that impact habitat quality, including competition, predation, water quality, substrate, and cover. Another factor that is very important in WWPs but is often overlooked in habitat suitability analyses is the large amount of recreational use, which can scare fish and disrupt spawning grounds. 3-D hydraulic variables could also play an important role in determining habitat quality. In the WWP pools, 2-D model results did not describe the spatial distribution of flow characteristics or the magnitude of variables as well as 3-D results. This thesis supports the use of 3-D modeling for complex flow found in WWPs, but projects should be evaluated case-by-case to determine if the simplified 2-D rendering of flow characteristics is acceptable. For 3-D modeling to be widely useful, improved understanding of linkages between 3-D aquatic habitat quality and hydraulic descriptors such as TKE, vorticity, and velocity is needed.

BIBLIOGRAPHY

- Belica, L. (2007), Brown Trout (*Salmo trutta*): A Technical Conservation Assessment, U. S. Department of Agriculture Forest Service, Rocky Mountain Region, Species Conservation Project, 118 p.; available: <http://www.fs.fed.us/r2/projects/scp/assessments/browntrout.pdf>.
- Bernstein, Y., and W. L. Montgomery (2008), Rainbow Trout (*Oncorhynchus mykiss*): A Technical Conservation Assessment, U. S. Department of Agriculture Forest Service, Rocky Mountain Region, Species Conservation Project, 83 p.; available: <http://www.fs.fed.us/r2/projects/scp/assessments/rainbowtrout.pdf>.
- Binns, N. A. (1994), Long-term responses of trout and macrohabitats to habitat management in a Wyoming headwater stream, *North American Journal of Fisheries Management*, **14**(1), 87–98.
- Booker, D. J., and M. J. Dunbar (2004), Application of Physical HABitat SIMulation (PHABSIM) modelling to modified urban river channels, *River Research and Applications*, **20**(2), 167–183.
- Booker, D. J., M. J. Dunbar, and A. Ibbotson (2004), Predicting juvenile salmonid drift-feeding habitat quality using a three-dimensional hydraulic-bioenergetic model, *Ecological Modelling*, **177**(1–2), 157–177.
- Bovee, K. D. (1982), A Guide to Stream Habitat Analysis Using the Instream Flow Incremental Methodology, U. S. Department of the Interior, Fish and Wildlife Service, Washington, DC, 248 p.
- Bovee, K. D., B. L. Lamb, J. M. Bartholow, C. B. Stalnaker, J. Taylor, and J. Henriksen (1998), Stream Habitat Analysis Using the Instream Flow Incremental Methodology, *Report*

- USGS/BRD/ITR-1998-0004, U. S. Department of the Interior, U. S. Geological Survey, Biological Resources Division, 131 p.
- Bremset, G. (2000), Seasonal and diel changes in behaviour, microhabitat use and preferences by young pool-dwelling atlantic salmon, *salmo salar*, and brown trout, *salmo trutta*, *Environmental Biology of Fishes*, **59**(2), 163–179.
- Carney, S. K., B. P. Bledsoe, and D. Gessler (2006), Representing the bed roughness of coarse-grained streams in computational fluid dynamics, *Earth Surface Processes and Landforms*, **31**(6), 736–749.
- Crowder, D. W., and P. Diplas (2000a), Evaluating spatially explicit metrics of stream energy gradients using hydrodynamic model simulations, *Canadian Journal of Fisheries and Aquatic Sciences*, **57**(7), 1497–1507.
- Crowder, D. W., and P. Diplas (2000b), Using two-dimensional hydrodynamic models at scales of ecological importance, *Journal of Hydrology*, **230**(3–4), 172–191.
- Crowder, D. W., and P. Diplas (2002), Vorticity and circulation: spatial metrics for evaluating flow complexity in stream habitats, *Canadian Journal of Fisheries and Aquatic Sciences*, **59**(4), 633–645.
- Edwards, E. A. (1983), Habitat Suitability Index Models: Longnose Sucker, *Report FWS/OBS-82/10.35*, U. S. Department of the Interior, Fish and Wildlife Service, September, 21 p.
- Edwards, E. A., H. Li, and C. B. Schreck (1983), Habitat Suitability Index Models: Longnose Dace, *Report FWS/OBS-82/10.33*, U. S. Department of the Interior, Fish and Wildlife Service, April, 13 p.
- Ergun, S. (1952), Fluid flow through packed columns, *Chemical Engineering Progress*, **48**, 89–94.
- Flow Science (2009), FLOW-3D User Manual: v9.4, Flow Science, Inc.

- Fox, B. (in prep), Fish passage in whitewater kayak parks, Thesis, Colorado State University, Department of Civil and Environmental Engineering, Fort Collins, CO.
- Ghanem, A., P. Steffler, F. Hicks, and C. Katopodis (1996), Two-dimensional hydraulic simulation of physical habitat conditions in flowing streams, *Regulated Rivers: Research & Management*, **12**(2–3), 185–200.
- Greenberg, L. A., and P. S. Giller (2001), Individual variation in habitat use and growth of male and female brown trout, *Ecography*, **24**(2), 212–224.
- Greenberg, L. A., T. Steinwall, and H. Persson (2001), Effect of depth and substrate on use of stream pools by Brown Trout, *Transactions of the American Fisheries Society*, **130**(4), 699–705.
- Hess, A. (2013), Personal Communication, Colorado State University, Department of Statistics.
- Kondratieff, M. (2013), Personal Communication, Colorado Parks and Wildlife.
- Kozarek, J., W. Hession, C. Dolloff, and P. Diplas (2010), Hydraulic complexity metrics for evaluating in-stream Brook Trout habitat, *Journal of Hydraulic Engineering*, **136**(12), 1067–1076.
- Lacey, R. W. J., and R. G. Millar (2004), Reach scale hydraulic assessment of instream salmonid habitat restoration, *Journal of the American Water Resources Association*, **40**(6), 1631–1644.
- Lacey, R. W. J., V. S. Neary, J. C. Liao, E. C. Enders, and H. M. Tritico (2012), The IPOS framework: linking fish swimming performance in altered flows from laboratory experiments to rivers, *River Research and Applications*, **28**(4), 429–443.
- Lamouroux, N., Y. Souchon, and E. Herouin (1995), Predicting velocity frequency distributions in stream reaches, *Water Resources Research*, **31**(9), 2367–2375.

- Lane, S. N., K. F. Bradbrook, K. S. Richards, P. A. Biron, and A. G. Roy (1999), The application of computational fluid dynamics to natural river channels: three-dimensional versus two-dimensional approaches, *Geomorphology*, **29**(1–2), 1–20.
- Larscheid, J. G., and W. A. Hubert (1992), Factors influencing the size structure of Brook Trout and Brown Trout in southeastern Wyoming mountain streams, *North American Journal of Fisheries Management*, **12**(1), 109–117.
- McGrath, C. C. (2003), Potential Effects of Whitewater Parks on In-stream Habitat, Recreational Engineering and Planning, Inc., Boulder, CO.
- Miller, W. J., and K. M. Swaim (2011), Final Instream Flow Report for the Colorado River from Kremmling, Colorado downstream to Dotsero, Colorado.
- Miller, W. J. (2013), Personal Communication.
- Olsen, N. R. B., and S. Stokseth (1995), Three-dimensional numerical modelling of water flow in a river with large bed roughness, *Journal of Hydraulic Research*, **33**(4), 571–581.
- Pasternack, G. B., M. K. Bounrisavong, and K. K. Parikh (2008), Backwater control on riffle–pool hydraulics, fish habitat quality, and sediment transport regime in gravel-bed rivers, *Journal of Hydrology*, **357**(1–2), 125–139.
- R Development Core Team (2012). R: A language and environment for statistical computing. R Foundation for Statistical Computing, Vienna, Austria, ISBN 3-900051-07-0; available: <http://www.R-project.org>.
- Rajaratnam, N., and C. Katopidis (1997), Hydraulics of resting pools for denil fishways, *Journal of Hydraulic Engineering*, **123**(7), 632.
- Raleigh, R. F., T. Hickman, R. C. Solomon, and P. C. Nelson (1984), Habitat Suitability Information: Rainbow Trout, *Report FWS/OBS-82/10.60*, U. S. Department of the Interior, Fish and Wildlife Service, January, 64 p.

- Raleigh, R. F., L. D. Zuckerman, and P. C. Nelson (1986), Habitat Suitability Index Models and Instream Flow Suitability Curves: Brown Trout, *Biological Report 82(10.124)* (revised), U. S. Department of the Interior, Fish and Wildlife Service, September, 65 p.
- RipBoard (2011), Whitewater parks and kayak play parks: great riverboarding near urban communities, RipBoard Inc., Denver, CO; available: www.ripboard.com/community/whitewaterpark.shtml.
- Rodriguez, J. F., F. A. Bombardelli, M. H. García, K. M. Frothingham, B. L. Rhoads, and J. D. Abad (2004), High-resolution numerical simulation of flow through a highly sinuous river reach, *Water Resources Management*, **18**(3), 177–199.
- Roni, P., K. Hanson, and T. Beechie (2008), Global review of the physical and biological effectiveness of stream habitat rehabilitation techniques, *North American Journal of Fisheries Management*, **28**(3), 856–890.
- Roni, P., and T. Beechie (2013), *Stream and Watershed Restoration: A Guide to Restoring Riverine Processes and Habitats*, Wiley-Blackwell, Hoboken, NJ.
- Shields, F. D., Jr., and J. R. Rigby (2005), River habitat quality from river velocities measured using acoustic doppler current profiler, *Environmental Management*, **36**(4), 565–575.
- Shuler, S., and R. Nehring (1993), Using the physical habitat simulation model to evaluate a stream habitat enhancement project, *Rivers*, **4**(3), 175–193.
- Silva, A. T., C. Katopodis, J. M. Santos, M. T. Ferreira, and A. N. Pinheiro (2012), Cyprinid swimming behaviour in response to turbulent flow, *Ecological Engineering*, **44**(0), 314–328.
- Thompson, D. M., J. M. Nelson, and E. E. Wohl (1998), Interactions between pool geometry and hydraulics, *Water Resources Research*, **34**(12), 3673–3681.

APPENDIX A DETAILED NUMERICAL MODELING METHODS

Sensitivity analyses were performed to test the effects of turbulence modeling, momentum advection, and uniform grid size on model resolution. The renormalized group model was chosen for turbulence closure because it performs well in situations with high shear and separation zones [Rodriguez *et al.*, 2004]. With this turbulence model, it is possible to specify the turbulence mixing length or have it dynamically computed. I tested the sensitivity of changing the mixing length on one simulation. I first calculated the maximum pool depth in that simulation, and then re-simulated nine times with the mixing length set to 10, 20, 30, 40, 50, 60, 70, 80, and 90% of the maximum depth. I found no substantial differences in velocity magnitudes and distributions, or in visible flow patterns, so I determined that a dynamically-computed mixing length was acceptable.

To test the momentum advection method, I ran one simulation with the default 1st order momentum advection and one simulation with 2nd order monotonicity momentum advection. Resulting depth, velocity, and flow patterns showed no substantial differences, so the 1st order method was chosen. This method requires substantially less computational time than the 2nd order method.

Finally, grid-size sensitivity was tested by incrementally reducing the size of the grid cells until the solution was grid-independent. Grid-independence was achieved when the head loss through the model domain changed less than 5% from the previous simulation. Most simulations achieved a head loss that was less than 2% different from the previous simulation, but there was not enough computational power to achieve this with all simulations. Final grid sizes for each simulation are summarized in Table A.1.

Table A.1. Cell size in FLOW-3D computational mesh for WWP reaches and natural reaches at all flow rates.

Reach	Flow Rate (cms)	Mesh Size		
		X-direction (cm)	Y-direction (cm)	Z-direction (cm)
WWP1	0.42	7.62	7.62	7.62
WWP2	0.42	7.62	7.62	7.62
WWP3	0.42	7.62	7.62	3.81
NR1-2 ^a	0.42	15.24	15.24	7.62
NR3	0.42	15.24	15.24	15.24
WWP1	4.25	7.62	7.62	7.62
WWP2	4.25	7.62	7.62	7.62
WWP3	4.25	7.62	7.62	7.62
NR1-2 ^a	4.25	15.24	15.24	7.62
NR3	4.25	15.24	15.24	15.24
WWP1	8.5	7.62	7.62	7.62
WWP2	8.5	7.62	7.62	7.62
WWP3	8.5	7.62	7.62	7.62
NR1-2 ^a	8.5	15.24	15.24	15.24
NR3	8.5	15.24	15.24	15.24

^a Reach NR1-2 includes NR1-A, NR1-B, and NR2

Roughness can be represented in three ways in a CFD model (Figure A.1). The first option is to use a fine grid that resolves all roughness elements. This method works when roughness elements are very large compared to the computational cell size. The second option is to use standard boundary laws, which assume a logarithmic velocity profile starting at the channel bed. This method works when the roughness is very small in comparison to the cell size, because the boundary equation is only applied to the computational cell closest to the bed. The third option is to approximate roughness using a porosity model, and is useful when the roughness elements vary in size or are in between the optimal sizes for the previous two methods [Olsen and Stokseth, 1995].

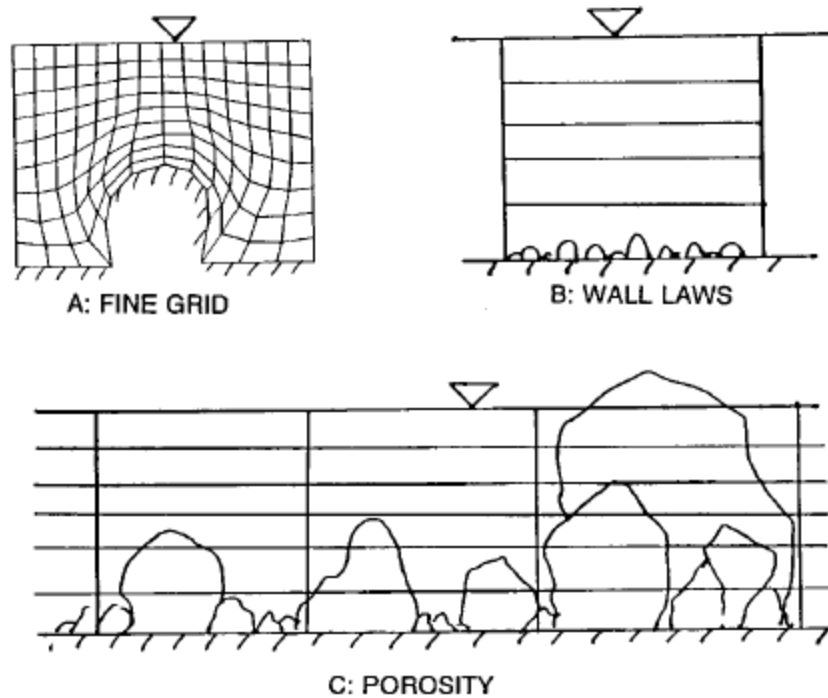


Figure A.1. Three ways of representing roughness in CFD models (from Olsen and Stokseth [1995]).

A porosity model was used to model the roughness in the natural reaches in this study. In FLOW-3D, I created a porous bed that was 30-cm thick. Below this was a solid bed with the same topography, ensuring that no water would be lost in the simulation. FLOW-3D uses the Forchheimer saturated drag model to calculate the flow through the porous region, and requires two drag coefficients as input [Flow Science, 2009]. These coefficients describe the relationship of the permeability of the media to the velocity, and are best described through experimental data [Flow Science, 2009]. Due to a lack of adequate data for the river system in this study, empirical correlations were used based on the Ergun [1952] Equation.

LIST OF ABBREVIATIONS

1-D	one-dimensional
2-D	two-dimensional
3-D	three-dimensional
ADCP	acoustic Doppler current profiler
ADV	acoustic Doppler velocimeter
CFD	computation fluid dynamics
CPW	Colorado Parks and Wildlife
CWI	Colorado Water Institute
GPS	Global Positioning System
HSI	Habitat Suitability Indices
LIDaR	LIGht Detection and Ranging
PHABSIM	Physical HABitat SIMulation
PIT	passive integrated transponder
®	registered
RANS	Reynolds-Averaged Navier-Stokes
RNG	renormalization group
STL	stereolithography
™	trademark
TKE	turbulent kinetic energy
VOF	volume of fluid
WWPs	whitewater parks
X, Y, Z	coordinates